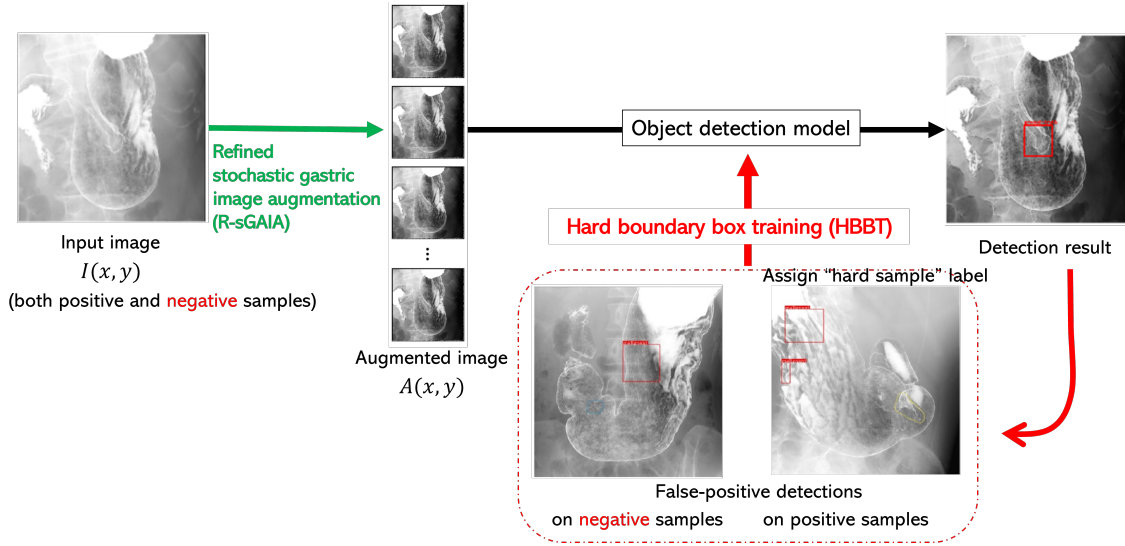


Graphical Abstract

Practical X-ray Gastric Cancer Screening Using Refined Stochastic Data Augmentation and Hard Boundary Box Training

Hideaki Okamoto, Quan Huu Cap, Takakiyo Nomura, Kazuhito Nabeshima, Jun Hashimoto, Hitoshi Iyatomi*



Highlights

Practical X-ray Gastric Cancer Screening Using Refined Stochastic Data Augmentation and Hard Boundary Box Training

Hideaki Okamoto, Quan Huu Cap, Takakiyo Nomura, Kazuhito Nabeshima, Jun Hashimoto, Hitoshi Iyatomi*

- We propose an unprecedented gastric cancer diagnostic support system for gastric X-rays, which can be performed by technicians, allowing more people to be screened compared to endoscopy, the current mainstream method that can only be performed by physicians. The system is based on a general deep learning-based object detection model and introduces two novel techniques: refined stochastic gastric image augmentation (R-sGAIA) and hard boundary box training (HBBT).
- A R-sGAIA is a probabilistic gastric fold region enhancement method that provides more learning patterns for cancer detection models.
- A HBBT is an efficient and versatile training method for common object detection models, enabling the use of unannotated negative (i.e., healthy control) samples that cannot be used in conventional detection models. This reduces false positives and improves overall performance.
- The proposed system achieves a sensitivity of 90.2% for gastric cancer, exceeding that of an expert (85.5%), with 42.5% of the detected candidate box regions showing cancerous lesions and a processing time of 0.51 seconds per image. It also achieves a 5.9-point higher F1 score compared to methods using the same object detection model and state-of-the-art data augmentation. The system efficiently guides radiologists on where to focus, significantly reducing their workload.
- Our R-sGAIA and HBBT are available at https://github.com/IyatomiLab/RsGAIA_HBBT/.

Practical X-ray Gastric Cancer Screening Using Refined Stochastic Data Augmentation and Hard Boundary Box Training

Hideaki Okamoto^a, Quan Huu Cap^{a,b}, Takakiyo Nomura^c, Kazuhito Nabeshima^c, Jun Hashimoto^c,
Hitoshi Iyatomi^{*a}

^a*Department of Applied Informatics, Graduate School of Science and Engineering, Hosei University, 3-7-2
Kajino, Koganei, 184-8584, Tokyo, Japan*

^b*AI Development Department, Aillis Inc., 2-2-1 Yaesu, Chuo, 104-0028, Tokyo, Japan*

^c*Department of Radiology, Tokai University School of Medicine, 143 Shimokasuya, Isehara, 259-1193, Kanagawa, Japan*

Abstract

Endoscopy is widely used to diagnose gastric cancer and has a high diagnostic performance, but it must be performed by a physician, which limits the number of people who can be diagnosed. In contrast, gastric X-rays can be performed by technicians and screen a much larger number of patients, but accurate diagnosis requires experience. We propose an unprecedented and practical gastric cancer diagnosis support system for gastric X-ray images, enabling more people to be screened. The system is based on a general deep learning-based object detection model and incorporates two novel techniques: refined probabilistic stomach image augmentation (R-sGAIA) and hard boundary box training (HBBT). R-sGAIA enhances the probabilistic gastric fold region, providing more learning patterns for cancer detection models. HBBT is an efficient training method that improves model performance by allowing the use of unannotated negative (i.e., healthy control) samples, which are typically unusable in conventional detection models. The proposed system achieves a sensitivity (SE) for gastric cancer of 90.2%, higher than that of an expert (85.5%). Additionally, two out of five detected candidate boxes are cancerous, maintaining high precision while processing images at a speed of 0.51 seconds per image. The system also outperforms methods using the same object detection model and state-of-the-art data augmentation, showing a 5.9-point improvement in the F1 score. In summary, this system efficiently identifies areas for radiologists to examine within a practical timeframe, significantly reducing their workload.

Declarations of interest: none

Keywords: Gastric cancer, X-ray, screening, data augmentation, hard negative mining, computer-aided diagnosis

1. Introduction

Gastric cancer is the third most deadly cancer globally, with a poor prognosis, especially in advanced stages (Rawla and Barsouk, 2019). However, early detection before metastasis can significantly improve outcomes, making early diagnosis and appropriate treatment crucial. Gastric cancer is primarily diagnosed through endoscopy or radiography. Endoscopy reports a sensitivity (SE) of 95.4%, which is superior to other methods, such as gastric radiography or X-ray, at 85.5% (Hamashima et al., 2013). However, endoscopy can only be performed by a physician, and the time and cost involved limit the

*Corresponding author

Email address: iyatomi@hosei.ac.jp (Hitoshi Iyatomi*)

number of people who can be screened. In contrast, gastric X-rays can be performed by radiographers, generating a large number of images, which makes this method suitable for mass screening – a significant advantage over endoscopic diagnosis. In Japan, a mass screening system was established, and in 2019, at least 3.87 million people underwent gastric X-rays for gastric cancer screening. Of these, 183,000 people were indicated for further testing, and 2,553 cases of gastric cancer were ultimately detected. By comparison, only 374,000 people underwent endoscopy for the same purpose (Matsuura, 2023). Although endoscopy’s effectiveness has led to a shift toward this diagnostic method, developing superior diagnostic support technology for gastric radiography would significantly contribute to the early detection and reduction of mortality from gastric cancer.

Gastric X-ray images are later interpreted by doctors to diagnose the stomach’s shape and mucosal atrophy (Uemura et al., 2001; Roder, 2002; Correa et al., 2004). An additional advantage of X-rays is their ability to reveal minute irregularities indicative of stage IIc lesions (early-stage tumors with slight indentations) – a subtle elevation within the indentation that lies beneath it. However, accurately reading these images requires a high level of skill, which many gastrointestinal radiologists may lack. When performed by a skilled physician, there is a high likelihood of assessing the extent of cancerous invasion deep within the surface of an early-stage cancer based on changes in the microscopic structure of the surface. The limitations of this diagnostic method lie in its dependence on extensive physician experience and the particular difficulty in detecting early-stage cancers, leading to a lower cancer detection capacity than that of endoscopy (Hibino et al., 2023). Therefore, there is a pressing need for an automated screening assistance system that can accurately and promptly detect gastric abnormalities from gastric X-ray images in clinical settings.

Healthy gastric folds are thin, smooth, and parallel; however, their thickness and size can be altered by gastric diseases such as inflammation, infection, ulcers, and tumors, leading to irregular bends, depressions, and tears in the lining mucosa (Correa et al., 2004). Most research on diagnostic support using gastric X-rays has focused on detecting gastritis, the precursor to gastric cancer, or the presence of *Helicobacter pylori* infection, which is believed to be a major cause of gastric cancer (Cooper et al., 1990; Kita, 1992; Minemoto et al., 2010; Nagano and Matsuo, 2010; Abe et al., 2014; Ishihara et al., 2015, 2017; Togo et al., 2019; Kanai et al., 2019, 2020). Among these studies, methods based on deep learning, particularly convolutional neural networks (CNNs), have shown excellent results in detecting gastritis. The main advantage of these deep learning techniques is their ability to automatically capture efficient features for the target task, which is promising in areas where disease features are difficult to define. However, studies directly detecting gastric cancer from radiographs are limited, despite the significance of gastric cancer diagnosis in terms of life expectancy. This may be because gastric cancer, especially in its early stages, is more difficult to diagnose compared to gastritis, where lesions often expand and develop to some degree. Reportedly, even with the latest machine learning techniques, distinguishing between gastritis and gastric cancer on endoscopic images—where signs of the disease are more visible – remains challenging (Horiuchi et al., 2020).

In the field of computer vision, CNN-based object detection methods (e.g., Faster R-CNN (Ren et al., 2015), YOLOv3 (Redmon and Farhadi, 2018), EfficientDet (Tan et al., 2020), and YOLOv7 (Wang et al., 2023)), which can simultaneously detect and classify the location of multiple objects in images, have been proposed and widely used. These methods are particularly valuable in medical applications because they not only detect regions of interest but also provide high explanatory power for the predicted results, as opposed to simply classifying images as benign or malignant (Hirasawa et al., 2018; Li et al., 2018; Okamoto et al., 2019; Laddha et al., 2019; Zhang et al., 2019). For instance, in a study on gastric X-ray images, Laddha et al. (2019) used YOLOv3 to automatically detect gastric polyps, achieving a mean average precision of 0.916. However, these object detection methods require precise annotation of lesion locations prior to training, which is extremely costly. To avoid high annotation

costs while still benefiting from the explanatory advantages of object detection models, previous studies on gastritis detection (Ishihara et al., 2017; Togo et al., 2019; Kanai et al., 2019, 2020) used patch-based CNNs, which only required image-level annotations. In the context of gastric cancer, where diagnostic challenges and outcomes are more severe, it is critical that physicians are able to interpret the results provided by diagnostic support systems.

With this motivation, we proposed a diagnostic support system that directly targets gastric cancer using X-ray images, which have rarely been studied, and offers high explanatory power for the results (Okamoto et al., 2019). Thanks to the proposed stochastic gastric image augmentation (sGAIA) based on medical knowledge, this system accurately represented candidate regions of gastric cancer within bounding boxes. In an evaluation using images from patients not included in the training set, the recall (SE) and precision of the detected bounding boxes were 92.3% and 32.4%, respectively. This recall is about 7% higher than that achieved by doctors (85.5%), and a box-by-box evaluation confirmed a true-to-false detection ratio of 1:3, which is sufficient for practical use. While the object detection model trained with sGAIA has reached a practical level of accuracy, further performance improvements are desirable. Currently, widely used object detection methods have the disadvantage of not being able to explicitly use negative (i.e., healthy control) data for training, in addition to the high cost of annotation. When such models are used for lesion detection, only images with lesions are used for training, while control images without lesions are excluded. This limitation presents an opportunity for improvement, which is a key focus of this study. In medical imaging, data are expensive, and we believe that actively using healthy control images for training can enhance the model’s overall ability to detect lesions, effectively reducing annotation costs while maintaining performance. In this study, we proposed a practical gastric cancer screening system that includes two new techniques: refined stochastic gastric image augmentation (R-sGAIA), an improvement of sGAIA (Okamoto et al., 2019), and hard boundary box training (HBBT), which enables the use of negative or healthy control images for training, a feature not previously utilized in object detection neural networks. To suppress high-confidence false positives predicted by the object detector, HBBT registers each of these boxes as a “hard-sample” class and retrains the model until predetermined convergence conditions are met. We investigated 4,724 gastric X-ray images obtained from 145 patients in a clinical setting and confirmed the practicality and effectiveness of the proposed system by evaluating gastric cancer detection performance using a subject-based five-fold cross-validation strategy.

The contributions of this study are as follows:

- We proposed an unprecedented gastric cancer diagnostic support system for gastric X-rays, which can be taken by technicians. As a result, this allows more people to be screened, rather than endoscopy, which is currently the mainstream but can only be performed by physicians. The system is based on a general deep learning-based object detection model and includes two novel technical proposals: R-sGAIA and HBBT.
- R-sGAIA is a probabilistic gastric fold region enhancement method used to provide more learning patterns for cancer detection models.
- HBBT is an efficient and versatile training method for common object detection models that allows the use of unannotated negative (i.e., healthy control) samples that otherwise cannot be used for training in conventional detection models. This reduces false positives and thus improves overall performance.
- The SE of the proposed system for gastric cancer (90.2%) exceeds that of the expert (85.5%), while 42.5% of the detected candidate box regions show cancerous lesions, with a processing time

of 0.51 s/image. It is 5.9 points higher on the F1 score compared to methods using the same object detection model and state-of-the-art data augmentation. In short, the system efficiently shows the radiologist where to look, greatly reducing the radiologist’s workload.

- Our R-sGAIA and HBBT are available at https://github.com/IyatomiLab/RsGAIA_HBBT/.

2. Related work

2.1. Diagnostic support using gastric X-ray images

In the 1990s, methods were proposed for effectively extracting the pattern of gastric folds by applying binarization as a preprocessing step and estimating the gastric region based on the position of the barium reservoir (Cooper et al., 1990; Kita, 1992). In the 2010s, more empirical studies began to focus on gastric folds (Minemoto et al., 2010; Nagano and Matsuo, 2010; Abe et al., 2014; Ishihara et al., 2015). Ishihara et al. (2015) calculated numerous statistical features (7,760 per case) for *H. pylori* infection, a major cause of gastric cancer, by analyzing post-infection mucosal patterns and gastric folds. Their support vector machine, trained on data from 2,100 patients (with eight images per person), achieved a SE of 89.5% and a SP of 89.6%.

More recently, deep learning techniques have been applied to the detection of gastritis using patch-based CNNs on gastric X-ray images (Ishihara et al., 2017; Togo et al., 2019; Kanai et al., 2019, 2020). Although these methods targeted gastritis, which is easier to diagnose than gastric cancer, they achieved high detection accuracy and were considered practical for diagnostic assistance. Kanai et al. (2020) used a patch-based CNN to detect *H. pylori*-associated chronic atrophic gastritis. They trained image patches from both the inside and outside of the stomach and made a diagnosis by taking a majority vote of each estimated result in the stomach region. Manual annotation of regions of interest (ROIs) prior to training, along with self-learning to increase the number of training patches, ultimately yielded a harmonic mean SE and SP of 95.5% for the test data from different patients. While excellent screening results have been achieved for gastritis, the detection of more serious and difficult-to-diagnose gastric cancers has not been well studied. In the case of gastric cancer, it is also crucial to provide an explanation for the results. The proposed method significantly improves upon our previous work on a gastric cancer detection system that can present explainable results (Okamoto et al., 2019), incorporating two new technical advancements.

2.2. Diagnostic support research for endoscopic images

In recent years, many methods for analyzing narrow-band endoscopy images to assist in diagnosing gastric cancer using deep learning technology have been proposed (Kanayama et al., 2019; Wu et al., 2019; Horiuchi et al., 2020; Li et al., 2020; Gong et al., 2023).

Wu et al. (2019) used classic VGG16 and ResNet-50 models, achieving a SE of 94.0% and a SP of 91.0% based on 24,549 images for diagnosing early gastric cancer. Li et al. (2020) employed an Inception-v3 model, achieving an SE of 91.2% and an SP of 90.6% based on 2,429 images of gastric magnification endoscopy with narrow-band imaging. Horiuchi et al. (2020) trained a GoogLeNet model with 1,499 images of gastric cancer and 1,078 images of gastritis, achieving an SE of 95.4%, an SP of 71.0%, and an area under the receiver operating characteristic (ROC) curve (AUC) of 0.852. Gong et al. (2023) developed a Convolution and Relative Self-Attention Parallel Network using 3,576 endoscopic images from 205 patients, reporting an F1 score of 0.948 in their experiments with a 7:3 split of training and test images. While these methods produce excellent results, none of them explicitly state whether the training dataset is completely separate from the patients whose images are in the evaluation set. This raises the possibility that images from the same patients were included in both the training and test

data, potentially leading to inflated performance scores due to the close similarity between the two datasets.

In contrast, Kanayama et al. (2019) constructed a diagnostic support system using 129,692 gastrointestinal endoscopy images with sophisticated CNN-based networks, including one synthesizer network and two different types of discriminator networks. Importantly, they ensured that images from the same patient were not divided between the training and evaluation sets, thus evaluating performance appropriately. They reported an average precision (AP) of 0.596 for cancer detection. Although the numerical performance of this method may seem lower, it is based on a newer and more sophisticated machine learning model than those used in previously reported methods, representing a more accurate diagnostic capability. They further enhanced their model by generating 20,000 high-resolution lesion images from 1,315 narrow-field-of-view images using their own generative adversarial network (Goodfellow et al., 2014) and adding these to the training set, improving the AP in cancer detection to 0.632. Shibata et al. (2020) constructed and rigorously evaluated a diagnostic model using Mask R-CNN on 1,208 images from 42 healthy subjects and 533 images from 93 unhealthy subjects (including gastric cancer). Their model achieved an SE of 96% for all tumor types, a false positive rate of 0.1/image, and an F1 score of 0.71 for gastric cancer. Ahmad et al. (2023) trained and evaluated a larger dataset than in previous studies (27,200 training and 6,800 testing images) with a novel approach that added Squeeze and Excitation attention blocks to YOLOv7 (Wang et al., 2023), achieving an F1 score of 0.71 (precision = 72%, recall = 69%).

While it is unclear whether proper data partitioning was employed, it is important to note that the number of images used was significantly larger than in other studies. Additionally, the use of more sophisticated methods yielded results different from earlier studies (which reported F1 scores around 90% or higher) where substantial data leakage was suspected. Given that the results were comparable to other reports (Shibata et al., 2020) with clearly distinct data partitions, it can be inferred that the data division was likely appropriate.

2.3. *Hard negative mining*

Hard sample or hard example mining, a technique that improves model performance by explicitly retraining the model on error-prone or hard-to-identify data (hard samples), is widely used in machine learning (Felzenszwalb et al., 2009; Shrivastava et al., 2016). It is particularly effective in addressing class imbalance and has been extensively applied, alongside metric learning, in tasks such as face or person detection from complex backgrounds (Zhang et al., 2016; Smirnov et al., 2018; Chen et al., 2020), among other applications.

In recent years, deep learning-based object detection models have also adopted this strategy, reporting significant performance improvements by relearning misdetected bounding box regions, including in the medical field (Li et al., 2019; Tang et al., 2019). However, such object detection models typically cannot utilize images that do not contain any detection targets (such as background images or healthy control images) for training, since the error function to be minimized is defined based on the position and size of the bounding box for each detection target. Existing hard sample mining methods have been applied to data with at least one annotation box of the target class and have used overdetected or undetected regions or image patches as hard samples. Our HBBT is a form of hard sample mining or hard negative mining, which retrains regions of false positives. However, it differs significantly in that it allows the use of healthy control cases, which could not be used in traditional object detection models, for training. This is a particularly important contribution in the medical field, where the cost of acquiring positive samples is high.

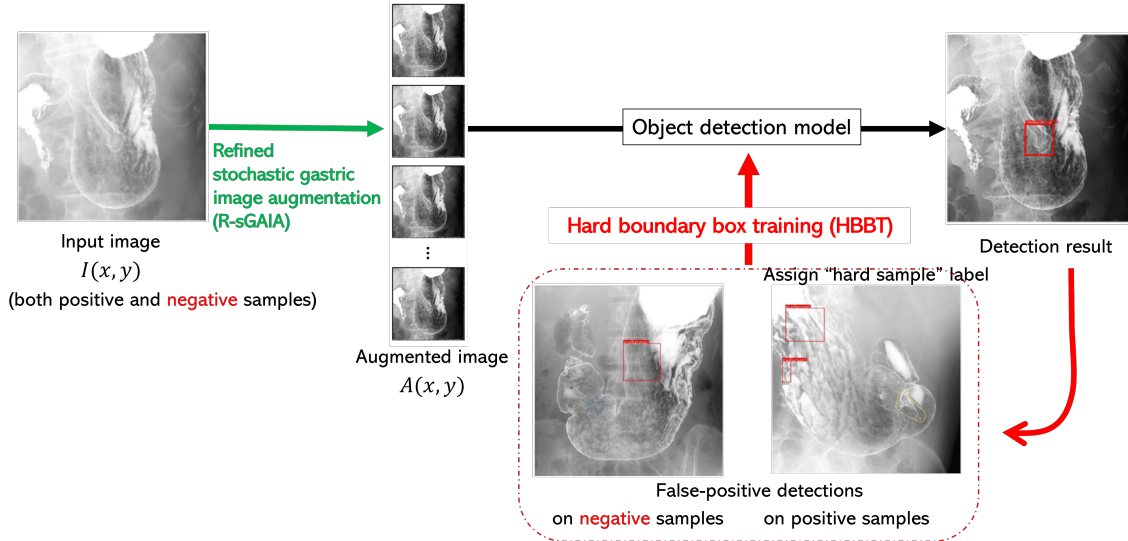


Figure 1: Overview of the proposed gastric cancer screening system.

3. Practical gastric cancer screening system

This study proposed a practical gastric cancer screening system using gastric X-ray images. The system highlights suspected cancerous sites with bounding boxes, allowing physicians to confirm the validity of the estimations. The two technical innovations in this study significantly improved system performance and achieved practical accuracy. The overall structure of the proposed system is shown in Figure 1. This study was approved by the Institutional Review Board of Tokai University Hospital (No. 20R-033, approval date: June 12, 2020). The main technical contributions were (1) R-sGAIA, which generates a diverse set of images that effectively emphasize the gastric fold region for data augmentation, and (2) HBBT, which reduces false positives by assigning “hard-sample” classes to bounding box regions where false positives are detected and iteratively learning from them. The object detection model used is EfficientDet (Tan et al., 2020), which incorporates EfficientNet (Tan and Le, 2019), a CNN known for its excellent performance, as its backbone, although the choice of model was arbitrary. The input images were $2,048 \times 2,048$ pixels, and the output consisted of a bounding box surrounding the presumed cancerous region in the image along with its confidence score.

3.1. R-sGAIA

The proposed R-sGAIA is a refined version of our previous method, sGAIA (Okamoto et al., 2019). Both R-sGAIA and sGAIA are probabilistic online data augmentation techniques designed to generate various images that highlight gastric folds in X-ray images, using medical knowledge to detect inflammation on the gastric mucosal surface. The original sGAIA improved gastric cancer detection by 6.9% in terms of F1-score (recall 92.3%, precision 32.4%) when applied to a Faster R-CNN model with ResNet-101 as the backbone, validating its effectiveness for practical screening. However, in sGAIA, the emphasis probability of each pixel $p(x, y)$, crucial for effective enhancement, was subjectively determined as a discrete value based on preliminary experiments. In the proposed R-sGAIA, $p(x, y)$ is instead modeled as a flexible continuous function, determined by only two hyperparameters. A schematic of the proposed R-sGAIA process is shown in Figure 2. Similar to sGAIA, R-sGAIA consists of four steps, with step 2 being the only difference.

- (Step 1) Calculation of edge strength $E(x, y)$

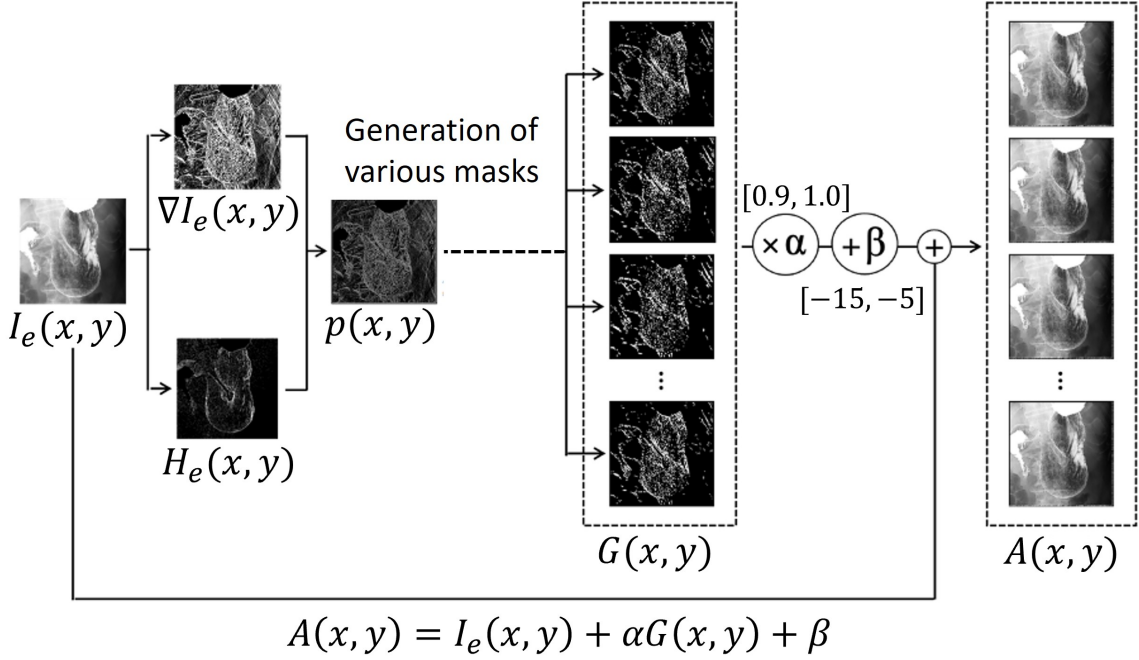


Figure 2: Overview of refined stochastic gastric image augmentation (R-sGAIA).

First, a contrast-enhanced image $I_e(x, y)$ is generated from the original gastric X-ray image $I(x, y)$ using histogram equalization. Then, its gradient and high-frequency components, $\nabla I_e(x, y)$, and $H_e(x, y)$, are obtained using general image processing techniques such as Canny edge detection filter and Butterworth high-pass filter, respectively. Each of them is normalized to $[0, 1]$, and the normalized edge strength $E(x, y)$ is calculated as follows:

$$E(x, y) = (\overline{\nabla I_e(x, y)} + \overline{H_e(x, y)})/2, \quad (1)$$

where $\overline{v(x, y)}$ is the linearly normalized value of $v(x, y)$ to $[0, 1]$.

- (Step 2) Calculation of the probability of a gastric fold region $p(x, y)$

The area of the edge of the gastric folds that is subject to augmentation is determined for each pixel as its probability $p(x, y)$. The proposed R-sGAIA differs from sGAIA in this step. In R-sGAIA, the edge intensity $e = E(x, y)$ of each pixel is used to obtain a probability map $p(x, y)$ of the gastric folds and edges using probabilities based on the sigmoid function defined below.

$$\begin{aligned} p(x, y) &= p(e) = p(E(x, y)) \\ &= \frac{1}{1 + \exp(-\gamma(E(x, y) - \theta))}. \end{aligned} \quad (2)$$

The parameters γ and θ are hyperparameters, respectively, defining the slope of the sigmoid function and adjusting the probability of running the augmentation of $E(x, y)$ to be 50%. They are determined based on the diagnostic performance of the validation data, as described below. Figure 3 compares the enhancement selection probability $p(e = E(x, y))$ based on the feature intensity e for R-sGAIA and sGAIA. Note that, in sGAIA, the probability $p(e)$ is subjectively determined based on preliminary experiments, as described above.

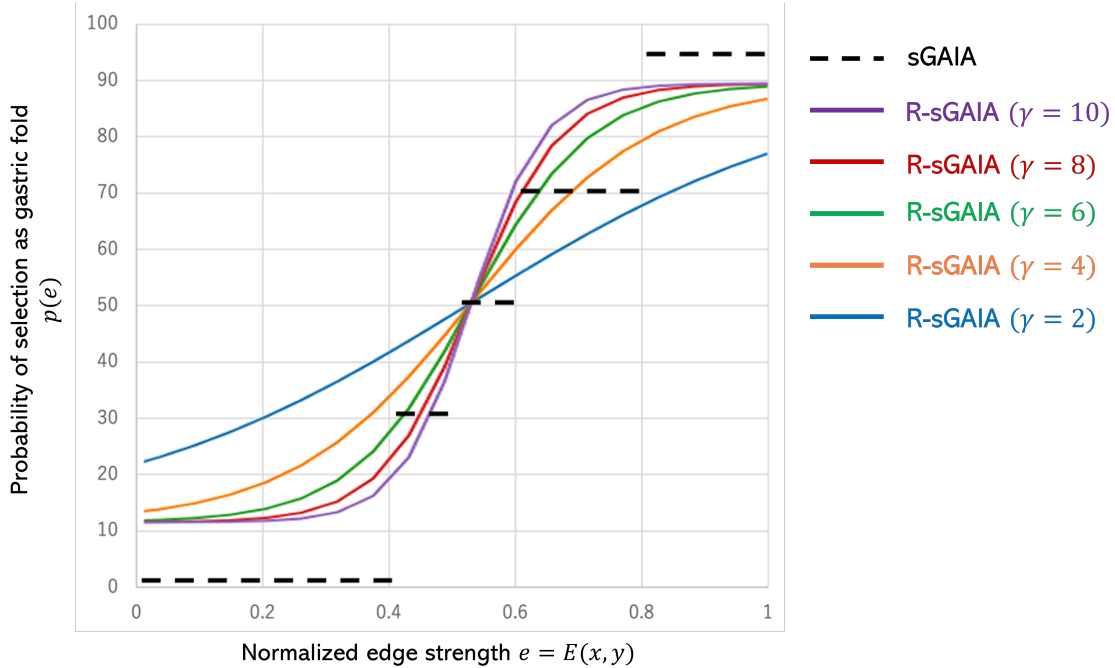


Figure 3: Probability of being detected as a gastric fold edge to be highlighted.

- (Step 3) Determination of gastric fold edge region $G(x, y)$

According to the probability map $p(x, y)$, a binary mask $G(x, y)$ of the gastric fold regions to be enhanced is determined by pixel-by-pixel sampling. Since this result is noisy, a morphological open operation is performed to remove many small isolated regions. $G(x, y)$ is created in such a way that a different mask is generated for each trial. This is the key to generating enhanced images of different gastric folds.

- (Step 4) Generation of enhanced gastric fold images $A(x, y)$

Finally, an enhanced gastric fold edge image $A(x, y)$ is obtained as follows:

$$A(x, y) = I_e(x, y) + \alpha G(x, y) + \beta. \quad (3)$$

Here, α and β are augmentation parameters. The value of α ranges from 0.9 to 1.0, and β ranges from -15 to -5 , with both values chosen randomly for each processing. Based on this, the proposed R-sGAIA probabilistically enhances the location and intensity of the gastric fold region each time, generating a different enhanced gastric image for each trial. This makes it highly compatible with online data augmentation in deep neural network training. Another significant advantage of R-sGAIA is that it does not require any additional runtime. We applied this R-sGAIA for online augmentation in training a machine learning model (EfficientDet-D7) used for cancer region detection.

3.2. HBBT

The diagnostic support system for gastric X-ray images is a one-class detection problem focused solely on positive (i.e., malignant) regions. However, our task involves many regions with similar image features, making them difficult to distinguish, even for experts. With a large number of training images, recent deep learning-based object detection algorithms can achieve the desired detection performance for

this task. However, this is challenging when labeled supervisory data is limited. Figure 4 shows typical false positives identified by experts in experiments using a vanilla detection model (i.e., EfficientDet-D7 without the proposed HBBT). The results indicate that most of these false positives fall into the five categories shown in examples (b)–(f) in Figure 4. However, it is difficult to clearly define and control these features in advance. In a fine-grained task like ours, it is crucial to reduce such hard negatives that exhibit high image similarity but are not the target. Note that our system detects a single class of candidate gastric cancer regions, with each detection box labeled as "malignant."

One promising approach to address this issue is hard sample mining, specifically hard negative mining, which aims to reduce over-detection and has been extensively studied, as mentioned earlier. However, training hard negative mining in object detection models typically focuses on reducing false positives (hard negatives) outside the target region in the training image. The data available for training are constrained by the object detection model, meaning that only images with some object detection annotation label can be used, unless a framework like semi-supervised learning is employed.

As mentioned earlier, a significant area for improvement in object detection models is the active use of negative samples, i.e., healthy controls. Conventional deep learning-based object detection algorithms typically only use images containing the object to be detected, excluding control cases without the object from training. This is a critical limitation. To address this, we propose HBBT, a simple yet effective method for suppressing false positives by incorporating the concept of hard negative mining. Training negative samples, which are more prone to false positives among the training data, is generally effective in constructing detectors with fewer false positives. In HBBT, as shown in Figure 1, the false-positive bounding boxes detected by the model are called hard boundary boxes. These are assigned hard-sample labels, converting the task into a two-class detection problem. The newly added hard-sample class label is treated as a negative example, and training is repeated until an optimal F1-score is achieved on the validation data. Importantly, this approach allows the use of not only positive data (e.g., images with cancerous regions) but also negative (i.e., healthy control) data, which are generally available in large quantities, for training by detecting and utilizing hard boundary boxes.

4. Experiments

4.1. Datasets and evaluation criteria

The image set used in this study consisted of 4,724 gastric X-ray images (1,117 images with 1,504 lesion annotations by radiologists and 3,607 images without lesions) from 145 patients in clinical settings, provided by the Tokai University School of Medicine, Japan. A total of 116 images from five randomly selected patients (49 of them with 49 annotated boxes) were used as validation data to determine the hyperparameters and to decide when to terminate HBBT. The remaining 4,608 images from 140 patients were used to train and evaluate the proposed system. Please note that we are not permitted to disclose the image data used in this experiment. Each image was an 8-bit grayscale with a resolution of $2,048 \times 2,048$ pixels. Based on expert annotations of the gastric cancer locations, the smallest rectangle surrounding each location was defined as a bounding box to be detected.

A subject-based five-fold cross-validation was used for training and evaluation, with precision, recall, and F1-score serving as the performance indicators for this system. The system provided candidate lesion bounding boxes, with their associated confidence scores exceeding a predefined detection threshold ξ . In the subject-based five-fold cross-validation, subjects were randomly divided into five groups. Images from four groups were used for training, while images from the remaining group were used for evaluation. This process was repeated five times, with a different group selected for evaluation each time. In medical research, including this experiment, data from the same subject can be inherently similar. Using standard cross-validation could lead to a virtual data leak, resulting in an overestimation

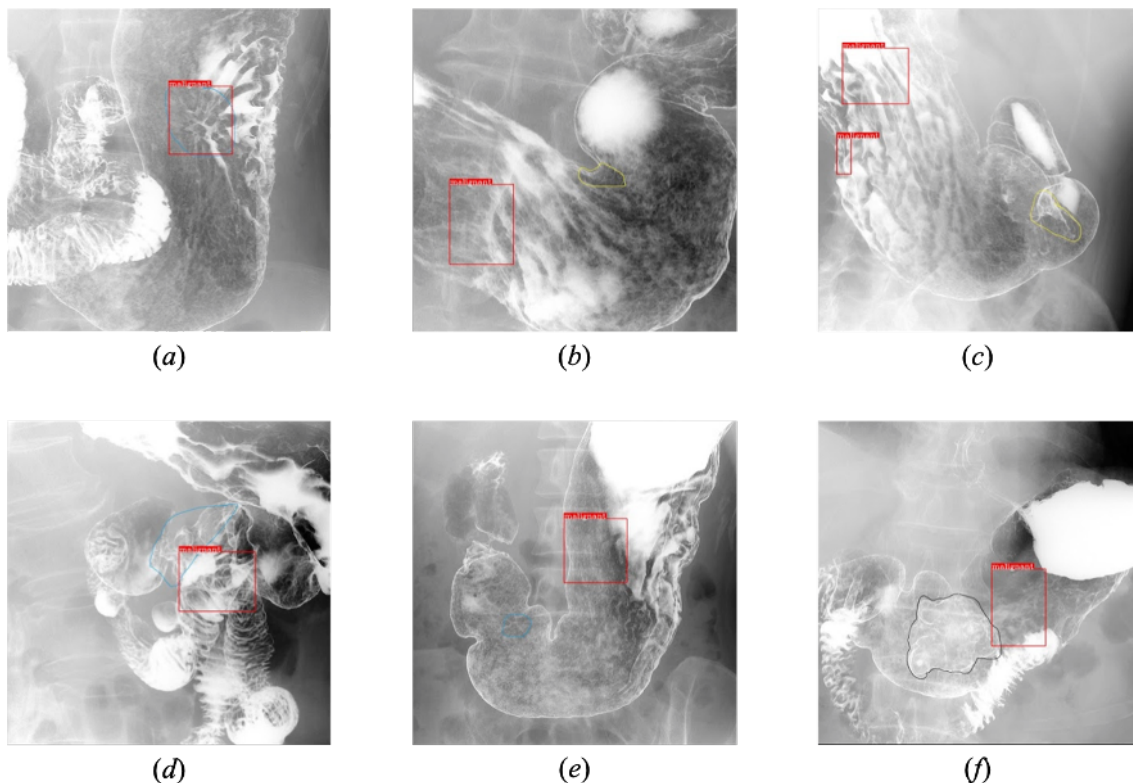


Figure 4: Positive example and five typical false positives provided by experts (as shown in red box).

(a) Positive example. (b) The area overlapping the osteophytes and spinous processes of the vertebral body. (c) Area where folds are gathered due to lack of air in the stomach. (d) Area where the duodenal Kerckring’s folds overlap with the stomach. (e) Areas where the mucosal surface of the stomach is irregular due to chronic gastritis. (f) Areas of advanced cancer that appear as wall changes rather than masses.

of model performance due to the similarity between training and test data. To prevent this and ensure a rigorous evaluation, we used this evaluation strategy.

4.2. Details of the detection model

We used EfficientDet-D7 (Tan et al., 2020) as a gastric cancer detection model with an input resolution of $1,536 \times 1,536$ pixels. One difference from the original image size was the margin for random cropping performed during training. The entire network was trained end-to-end, allowing it to simultaneously estimate the detection target at any location and size within the input image and classify its content (i.e., ‘cancer’). For details on the model, please refer to the original paper. The learning rate was set to 0.001, with a batch size of 32 and 100 training epochs. The optimization method used was momentum SGD (Qian, 1999), with the exponential decay rate of the first-order moment set to 0.9. To construct the proposed gastric cancer detection system, we applied the proposed R-sGAIA as an online augmentation technique during training. Additionally, healthy control images without cancer lesions, which are typically not used in general object detection models, were incorporated into the training process using HBBT.

Table 1: Detection performance in validation images for determining hyperparameter γ .

γ	Precision (%)	Recall (%)	F1-score
2	35.7	89.6	0.511
4	39.6	91.7	0.553
6	31.2	91.7	0.466
8	32.8	89.6	0.480
10	30.3	89.6	0.453

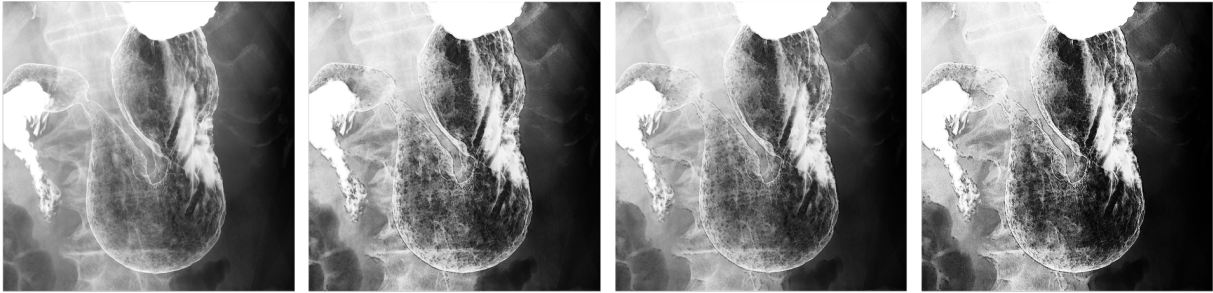


Figure 5: Example of augmented images (leftmost: original, others: enhanced images with R-sGAIA).

4.3. Experimental conditions

4.3.1. Determination of hyperparameters in R-sGAIA

In this section, we describe the hyperparameters θ and γ of the proposed R-sGAIA. θ is a hyperparameter that determines the edge strength $E(x, y)$ for which the probability of being considered a gastric fold is 50% in the sigmoid function $p(e = E(x, y))$ and was determined to be 0.55 based on the distribution of validation results. For γ , which characterizes the slope of $p(e)$, we selected $\gamma = 4$ from 2, 4, 6, 8, and 10 (Table 1) from the detection performance on validation images.

4.3.2. Detection of suspicious cancerous regions

To confirm the effectiveness of the proposed system with R-sGAIA and HBBT, we conducted comparative experiments using the following combinations of conditions. Since there is no directly comparable literature on gastric cancer detection, we implemented Laddha et al.’s (2019) method based on YOLOv3 and compared the performance on our task.

- Model selection

We selected two deep learning-based object detection models for this task: ResNet-101+Faster R-CNN (model 1) and EfficientDet-D7 (model 2). The first model has been widely used in the literature, including in sGAIA studies. The second model is one of the advanced object detection models frequently employed in many studies, although newer models have since been proposed. The training images used in the experiment to detect candidate cancer regions were grayscale, not color images, and since there was no suitable pre-trained model available, we trained the model from scratch using He’s initial weights He et al. (2015) with the random seed set to ’2021’. RandAugment (Cubuk et al., 2020), one of the state-of-the-art online augmentation methods, was applied to these models and served as the baseline for each (i.e., baseline models 1 and 2, respectively). Color augmentation was omitted because this task involves grayscale images. Based

on the detection performance of the validation dataset, 4 of the 13 augment types were selected with an intensity level of 3 (i.e., $M = 4$ and $N = 3$ according to their notation).

- Comprehensive evaluation of the proposals

We compared the performance of each model with and without the proposed techniques. For data augmentation, we used either RandAugment, conventional sGAIA (+sGAIA), or the proposed R-sGAIA (+R-sGAIA). The use of the proposed HBBT was indicated as either applied (+HBBT) or not.

4.3.3. Computational environment for model training and evaluation

In all experiments, we used a computer equipped with a Xeon E5-2650v4 2.2GHz CPU, 256GB of memory, and a GeForce RTX 2080 Ti GPU, running on Ubuntu 20.04 LTS. PyTorch was used as the deep learning framework. The implementations of Faster R-CNN¹, EfficientDet², and RandAugment³ were sourced from the links provided. Please note that the OS versions listed here reflect those in use at the time of the initial submission and are not the latest versions.

5. Results

Figure 5 shows an example of the augmented image obtained with the proposed R-sGAIA for the leftmost original image. Figure 6 compares cancer detection on the EfficientDet-D7 network (baseline model 2) with and without the proposed R-sGAIA and HBBT. The input images are shown in (a), the detection results with RandAugment in (b), and those with the proposed R-sGAIA+HBBT in (c). The proposed system (c) accurately detected the gastric cancer region without being affected by mucosal irregularities or small areas, as demonstrated in the top and middle rows. However, as shown in the bottom row, the result nearly covers the ROI but is slightly misaligned, leading to a false-positive evaluation.

The detection performance of gastric cancer regions from gastric X-ray images is summarized in Table 2. The object detection model detects regions where the probability (i.e., the confidence score) of belonging to the class of interest exceeds a predefined detection threshold of the bounding box ξ as locations containing objects of that class. HBBT assigns new negative labels to the over-detected regions that exceed the threshold ξ and retrains the model. Therefore, to draw an ROC curve for evaluation, the model must be trained every time ξ is changed, which is expensive. In this experiment, therefore, the detection threshold ξ was determined such that the SE (= recall) of detecting gastric cancer was about 90%, which was higher than the doctor’s 85.5%. At this detection threshold, HBBT improves precision by 2.3 points in Faster R-CNN (baseline model 1) and 3.3 points in EfficientDet-D7 (baseline model 2). Our system, using the proposed techniques, R-sGAIA and HBBT, achieved a recall of 90.2%, a precision of 42.5%, and an F1-score of 0.578 (Table 2).

The combination of the proposed R-sGAIA and HBBT showed a significant improvement over RandAugment, one of the most advanced data augmentations, in the detection of gastric cancer using the general object detection model. Specifically, the improvement was 10.3 points and 6.1 points in precision, and 10.9 points and 5.9 points in F1 scores for Faster R-CNN (model 1) and EfficientDet-D7 (model 2), respectively.

The processing time required for one X-ray image is approximately 0.51 seconds, making the proposed system a practical and efficient screening tool for gastric X-ray images.

¹https://pytorch.org/vision/master/models/faster_rcnn.html

²<https://github.com/rwightman/efficientdet-pytorch>

³<https://pytorch.org/vision/main/generated/torchvision.transforms.RandAugment.html>

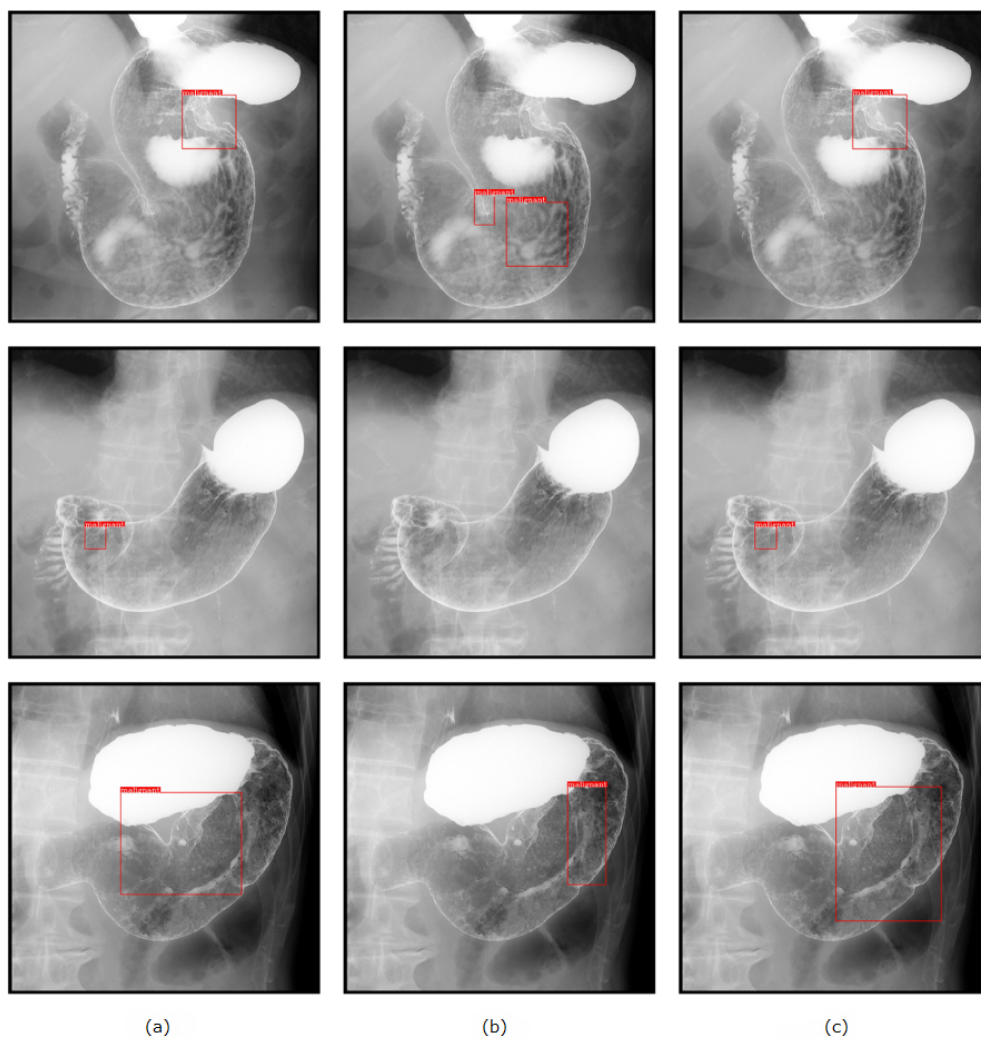


Figure 6: Example of cancer detection on EfficientDet-D7 networks (as shown in red box): (a) ground-truth region, (b) results obtained with RandAugment (baseline model 2), and (c) those with R-sGAIA+HBBT (proposed). The proposed R-sGAIA+HBBT led to the accurate detection for the top and middle examples, whereas for the bottom result, although it showed some improvement, the detection was inaccurate.

6. Discussion

The cancer detection performance of the proposed system in this study was significantly better than that achieved using baseline methods, including RandAugment (a state-of-the-art general data augmentation strategy), existing methods such as sGAIA Okamoto et al. (2019), and those proposed by (Laddha et al., 2019). Additionally, the system’s cancer detection capability exceeded that of a physician’s reading ($\sim 85.5\%$). In more than 2 out of 5 cases, the detection results presented by the system were cancerous. For a physician using the system, this means that by simply checking the areas surrounded by the few bounding boxes presented in a gastric X-ray image, a higher diagnostic yield can be achieved than with a conventional reading. In other words, the system is practically effective for on-site medical examinations and can significantly reduce the burden on physicians.

Table 2: Comparison of the detectability of gastric cancer sites.

	Augmentation			HBBT	Precision	Recall	F1-score
	RandAug [†]	sGAIA [‡]	R-sGAIA				
Laddha et al. (2019)*					26.5	89.7	0.409
Model 1 (Faster R-CNN on ResNet101)							
+ RandAugment (baseline model 1)	✓				28.4	90.1	0.432
+ sGAIA		✓			33.8	90.4	0.492
+ R-sGAIA			✓		36.4	90.2	0.519
+ R-sGAIA + HBBT (proposed)			✓	✓	38.7	90.1	0.541
Model 2 (EfficientDet-D7)							
+ RandAugment (baseline model 2)	✓				36.4	90.5	0.519
+ sGAIA		✓			37.9	90.1	0.534
+ R-sGAIA			✓		39.2	90.2	0.546
+ HBBT	✓			✓	39.4	89.9	0.548
+ R-sGAIA + HBBT (proposed)			✓	✓	42.5	90.2	0.578

* originally used for gastric polyp detection with YOLOv3 (Redmon and Farhadi, 2018).

[†] RandAugment (Cubuk et al., 2020) with $M = 4$ and $N = 3$.

[‡] sGAIA (Okamoto et al., 2019).

6.1. R-sGAIA

The proposed R-sGAIA can probabilistically highlight the gastric folds on a pixel-by-pixel basis based on medical findings, as shown in Figure 5. In this study, we found that R-sGAIA achieved an F1-score improvement of 6.0 points and 2.7 points over RandAugment on baseline models 1 and 2, respectively. This highlights the importance of probabilistic augmentation informed by medical knowledge. In baseline model 2, R-sGAIA further improved the F1-score by 1.2 points over the previous sGAIA in a direct comparison. This improvement may be attributed to R-sGAIA’s use of validation data to determine $p(e)$ as a continuous function, enabling it to generate a wider variety of enhancement images that better highlighted the gastric folds compared to sGAIA, which used a subjectively fixed value. The function of $p(e)$ with respect to edge strength $e = E(x, y)$ ranged approximately between 0.1 and 0.9, which likely contributed to the performance improvement. By allowing more stochastic variation in regions with very strong and weak edge strengths, R-sGAIA enhanced the diversity of the generated images, leading to better detection performance.

6.2. HBBT

Recent state-of-the-art object detection models (e.g., YOLOv7 (Wang et al., 2023)) are trained to minimize the difference between the boxes specified in the training data and the currently detected boxes, both in terms of their classes (i.e., contents) and locations. In other words, the model’s error is the sum of the class error and position error for each box, and training is performed to minimize these errors.

The proposed HBBT introduces a new and effective strategy that allows learning from healthy control images, which cannot be used to train conventional object detection models. It retrains over-detected boxes by assigning them a unique “hard-sample” class label to suppress future false detections. The HBBT strategy increases the class error for error-prone regions (i.e., hard samples) and retrains the model to reduce false positives. In essence, the HBBT learning algorithm is a strategy to reduce generic errors in object detection models, rather than focusing on the specific type of model. Furthermore,

HBBT actively incorporates negative samples, such as images of healthy controls, which are typically excluded from training by conventional object detection models.

Although HBBT is a simple method that recursively learns to eliminate false positives detected in images, including control images, it alone improves precision by 2.3 points and 3.3 points and F1-score by 4.9 points and 2.9 points on baseline models 1 and 2, respectively. HBBT is a general-purpose learning method that can be combined with any object detection algorithm, not just for gastric cancer detection, as demonstrated in this study. Since the final model detection is determined by the bounding box confidence threshold, HBBT not only reduces the number of false positives but also helps minimize false negatives (as seen in the middle case in Figure 6).

6.3. For practical screening

In this diagnostic support system, the ability to handle the diversity in size and shape of the tumor area to be detected depends on the detectability of the object detection model used. The range of object sizes that can be detected is determined by hyperparameters such as anchor size and aspect ratio. In the task of cancer detection from gastric X-ray images, the general settings of the object recognition model are sufficient, as the images are taken in a way that ensures the tumor size is large enough for visual diagnosis by a physician. However, for extremely small tumors, it is necessary to adjust hyperparameters to account for their size.

Since R-sGAIA is an online data augmentation method and HBBT is a training method, they do not impact the execution time of the diagnostic process. The current processing time of 0.5 seconds per image is considered sufficiently practical, and further improvements to the detection model are expected to increase speed in the future.

Detecting gastric cancer regions from X-ray images is inherently challenging, not only for automatic diagnostic systems but also for experts. Despite these challenges, our two technological innovations, R-sGAIA and HBBT, have significantly improved the detection performance of gastric cancer, achieving a level of performance and speed that can be effectively used by physicians as a diagnostic aid. Our diagnostic support system offers a concrete solution to the challenges of gastric radiography, which has been easy to acquire images but difficult to diagnose. In the future, we aim to work closely with experts to further refine and improve the system.

6.4. Comparison with automated diagnostic support methods for other modalities

Many diagnostic support studies have focused on endoscopy, the most commonly used method for diagnosing gastric cancer. However, as mentioned earlier, most of these studies did not properly separate the training data from the evaluation data, leading to data leakage and artificially inflated diagnostic performance. Recent studies that have addressed this issue by using more sophisticated machine learning methods (Shibata et al., 2020; Ahmad et al., 2023) have reported detection performance for gastric cancer with an image-based F1 score of approximately 0.7, which is considered the current standard for diagnostic accuracy.

Due to its noninvasiveness and ability to image the entire body, X-ray computed tomography (CT) is widely used for detecting not only gastric cancer but also other organs and diseases. Diagnostic studies of gastric cancer using CT typically rely on classical radiomics, including necessary pre-treatment steps. Depending on the cancer stage, diagnostic performance usually achieves an AUC of 0.7 to 0.8 (Meng et al., 2020; Huang et al., 2022). The application of deep learning in this context primarily focuses on predicting patient prognosis and segmenting tumor areas rather than directly diagnosing cancer. Hao et al. (2022) demonstrated that radiomic features and machine learning-extracted features (i.e., low-dimensional representations) are effective in predicting the prognosis of gastric cancer patients, indicating that these techniques will become more prevalent in the future.

While the diagnostic performance of these automated support methods may appear lower than the 95% SE reported by physicians for gastric cancer, it is essential to note that this comparison is patient-based, making direct comparisons challenging. As automated diagnostic methods are introduced into clinical practice, their actual performance is likely to approach the current SE of physicians, particularly when multiple outputs are integrated to inform a final decision, providing significant support to physicians. Although our F1 score of 0.578 for the diagnostic performance of gastric X-ray images may seem lower than that of other modalities, it is important to recognize that this is a box-based evaluation. Additionally, since physicians diagnose gastric cancer by reviewing multiple images during a gastric X-ray examination, our method’s ability to highlight the ROI in each image makes it highly valuable. Furthermore, our approach is significant as it represents the first use of gastric X-ray images to aid in the diagnosis of gastric cancer.

6.5. Limitations of the study

In recent years, it has become apparent that medical images, such as MR images, contain features unique to each facility due to differences in imaging equipment, protocols, geometry, and other factors. These so-called domain differences can significantly impact the results of machine learning tasks, such as classification, when applied without adjustment. The gastric X-ray images used in this study were exclusively taken at medical facilities affiliated with Tokai University. While domain differences may affect the analysis of gastric X-ray images obtained from different facilities, this has not been verified in this study.

7. Conclusions

In this paper, we have proposed an unprecedented, accurate, and fast gastric cancer screening system from gastric X-ray images, built on two key innovations: (1) R-sGAIA and (2) HBBT. The proposed system (R-sGAIA + HBBT on the EfficientDet-D7 network) achieves a SE of 90.2%, surpassing that of physicians (85.5%), with a processing time of approximately 0.5 seconds per image. Notably, 42.5% of the detected candidate box regions contain cancer, meaning our system effectively narrows down the areas that physicians need to examine. This system also achieves an F1 score 5.9 points higher than the same network using RandAugment, a state-of-the-art data augmentation method. Diagnosing gastric cancer using gastric X-rays is a challenging task that requires extensive experience. We hope that our proposal will assist in diagnosis, leading to early detection and a reduction in the number of deaths in the near future.

Acknowledgments

This research was supported in part by the Ministry of Education, Science, Sports and Culture of Japan (JSPS KAKENHI), Grant-in-Aid for Scientific Research (C), 22K07728, 2022–2024. No financial support was received that would have influenced the results of this study.

H. Okamoto was responsible for the practical system development of the study and the writing of the paper; T. Nomura, K. Nabeshima, and J. Hashimoto provided medical guidance, data collection, diagnosis, and other insights; and J. Hashimoto and H. Iyatomi were responsible for the study design, overall management, and writing of the paper.

References

Abe, K., Nakagawa, H., Minami, M., Tian, H., 2014. Features for discriminating normal cases in mass screening for gastric cancer with double contrast X-ray images of stomach. *Journal of Biomedical Engineering and Medical Imaging* 1.

- Ahmad, S., Kim, J.S., Park, D.K., Whangbo, T., 2023. Automated detection of gastric lesions in endoscopic images by leveraging attention-based yolov7. *IEEE Access* .
- Chen, K., Chen, Y., Han, C., Sang, N., Gao, C., 2020. Hard sample mining makes person re-identification more efficient and accurate. *Neurocomputing* 382, 259–267.
- Cooper, J., Khan, G., Taylor, G., Tickle, I., Blundell, T., 1990. X-ray analyses of aspartic proteinases: II. Three-dimensional structure of the hexagonal crystal form of porcine pepsin at 2.3 Å resolution. *Journal of Molecular Biology* 214, 199–222.
- Correa, P., Piazuolo, M.B., Camargo, M.C., 2004. The future of gastric cancer prevention. *Gastric Cancer* 7, 9–16.
- Cubuk, E.D., Zoph, B., Shlens, J., Le, Q.V., 2020. RandAugment: Practical automated data augmentation with a reduced search space, in: *Proceedings of the IEEE/CVF Conference on Computer Vision and Pattern Recognition Workshops*, pp. 702–703.
- Felzenszwalb, P.F., Girshick, R.B., McAllester, D., Ramanan, D., 2009. Object detection with discriminatively trained part-based models. *IEEE Transactions on Pattern Analysis and Machine Intelligence* 32, 1627–1645.
- Gong, D., Yan, L., Gu, B., Zhang, R., Mao, X., He, S., 2023. A computer-assisted diagnosis system for the detection of chronic gastritis in endoscopic images using a novel convolution and relative self-attention parallel network. *IEEE Access* 11, 116990–117003.
- Goodfellow, I., Pouget-Abadie, J., Mirza, M., Xu, B., Warde-Farley, D., Ozair, S., Courville, A., Bengio, Y., 2014. Generative adversarial nets. *Advances in Neural Information Processing Systems* 27.
- Hamashima, C., Okamoto, M., Shabana, M., Osaki, Y., Kishimoto, T., 2013. Sensitivity of endoscopic screening for gastric cancer by the incidence method. *International Journal of Cancer* 133, 653–659.
- Hao, D., Li, Q., Feng, Q.X., Qi, L., Liu, X.S., Arefan, D., Zhang, Y.D., Wu, S., 2022. Identifying prognostic markers from clinical, radiomics, and deep learning imaging features for gastric cancer survival prediction. *Frontiers in oncology* 11, 725889.
- He, K., Zhang, X., Ren, S., Sun, J., 2015. Delving deep into rectifiers: Surpassing human-level performance on imagenet classification, in: *2015 IEEE International Conference on Computer Vision (ICCV)*, pp. 1026–1034. doi:10.1109/ICCV.2015.123.
- Hibino, M., Hamashima, C., Iwata, M., Terasawa, T., 2023. Radiographic and endoscopic screening to reduce gastric cancer mortality: a systematic review and meta-analysis. *The Lancet Regional Health–Western Pacific* 35, 100741.
- Hirasawa, T., Aoyama, K., Tanimoto, T., Ishihara, S., Shichijo, S., Ozawa, T., Ohnishi, T., Fujishiro, M., Matsuo, K., Fujisaki, J., et al., 2018. Application of artificial intelligence using a convolutional neural network for detecting gastric cancer in endoscopic images. *Gastric Cancer* 21, 653–660.
- Horiuchi, Y., Aoyama, K., Tokai, Y., Hirasawa, T., Yoshimizu, S., Ishiyama, A., Yoshio, T., Tsuchida, T., Fujisaki, J., Tada, T., 2020. Convolutional neural network for differentiating gastric cancer from gastritis using magnified endoscopy with narrow band imaging. *Digestive Diseases and Sciences* 65, 1355–1363.

- Huang, H., Xu, F., Chen, Q., Hu, H., Qi, F., Zhao, J., 2022. The value of CT-based radiomics nomogram in differential diagnosis of different histological types of gastric cancer. *Physical and Engineering Sciences in Medicine* 45, 1063–1071.
- Ishihara, K., Ogawa, T., Haseyama, M., 2015. Helicobacter pylori infection detection from multiple X-ray images based on combination use of support vector machine and multiple kernel learning, in: 2015 IEEE International Conference on Image Processing (ICIP), IEEE. pp. 4728–4732.
- Ishihara, K., Ogawa, T., Haseyama, M., 2017. Detection of gastric cancer risk from X-ray images via patch-based convolutional neural network, in: 2017 IEEE International Conference on Image Processing (ICIP), IEEE. pp. 2055–2059.
- Kanai, M., Togo, R., Ogawa, T., Haseyama, M., 2019. Gastritis detection from gastric X-ray images via fine-tuning of patch-based deep convolutional neural network, in: 2019 IEEE International Conference on Image Processing (ICIP), IEEE. pp. 1371–1375.
- Kanai, M., Togo, R., Ogawa, T., Haseyama, M., 2020. Chronic atrophic gastritis detection with a convolutional neural network considering stomach regions. *World Journal of Gastroenterology* 26, 3650.
- Kanayama, T., Kurose, Y., Tanaka, K., Aida, K., Satoh, S., Kitsuregawa, M., Harada, T., 2019. Gastric cancer detection from endoscopic images using synthesis by GAN, in: *Medical Image Computing and Computer Assisted Intervention–MICCAI 2019: 22nd International Conference, Shenzhen, China, October 13–17, 2019, Proceedings, Part V* 22, Springer. pp. 530–538.
- Kita, Y., 1992. Model-driven contour extraction for physically deformed objects-application to analysis of stomach X-ray images, in: 1992 11th IAPR International Conference on Pattern Recognition, IEEE Computer Society. pp. 280–284.
- Laddha, M., Jindal, S., Wojciechowski, J., 2019. Gastric polyp detection using deep convolutional neural network, in: *Proceedings of the 2019 4th International Conference on Biomedical Imaging, Signal Processing*, pp. 55–59.
- Li, L., Chen, Y., Shen, Z., Zhang, X., Sang, J., Ding, Y., Yang, X., Li, J., Chen, M., Jin, C., et al., 2020. Convolutional neural network for the diagnosis of early gastric cancer based on magnifying narrow band imaging. *Gastric Cancer* 23, 126–132.
- Li, M., Wu, L., Wiliem, A., Zhao, K., Zhang, T., Lovell, B., 2019. Deep instance-level hard negative mining model for histopathology images, in: *Medical Image Computing and Computer Assisted Intervention–MICCAI 2019: 22nd International Conference, Shenzhen, China, October 13–17, 2019, Proceedings, Part I* 22, Springer. pp. 514–522.
- Li, Z., Wang, C., Han, M., Xue, Y., Wei, W., Li, L.J., Fei-Fei, L., 2018. Thoracic disease identification and localization with limited supervision, in: *Proceedings of the IEEE conference on computer vision and pattern recognition*, pp. 8290–8299.
- Matsuura, T., 2023. 2019 gastrointestinal cancer screening national aggregate report (in japanese). *Journal of Japanese Society of Gastroenterology (Nippon Shokakibyo Gakkai Zasshi)* 61, 86–101. doi:10.11404/jsgcs.61.86.

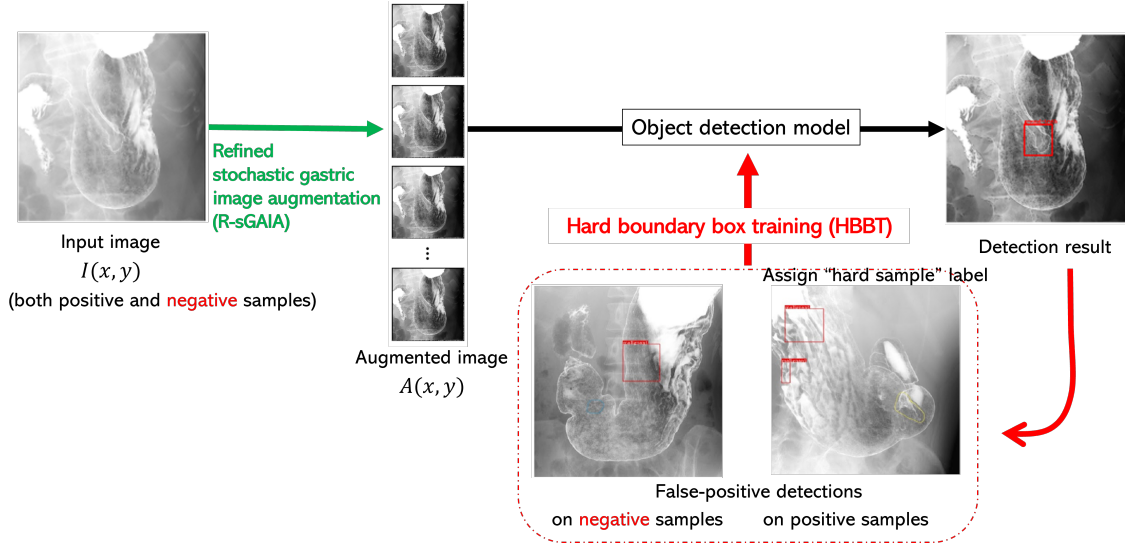
- Meng, L., Dong, D., Chen, X., Fang, M., Wang, R., Li, J., Liu, Z., Tian, J., 2020. 2d and 3D ct radiomic features performance comparison in characterization of gastric cancer: a multi-center study. *IEEE journal of biomedical and health informatics* 25, 755–763.
- Minemoto, T., Odama, S., Saitoh, A., Isokawa, T., Kamiura, N., Nishimura, H., Ono, S., Matsui, N., 2010. Detection of tumors on stomach wall in X-ray images, in: *International Conference on Fuzzy Systems*, pp. 1–5. doi:10.1109/FUZZY.2010.5584879.
- Nagano, N., Matsuo, T., 2010. Computer-aided diagnosis of gastrointestinal radiographs using adaptive differential filter and level set method, in: *Proceedings of the 2010 International Conference on Modelling, Identification and Control*, IEEE. pp. 442–447.
- Okamoto, H., Cap, Q.H., Nomura, T., Iyatomi, H., Hashimoto, J., 2019. Stochastic gastric image augmentation for cancer detection from X-ray images, in: *2019 IEEE International Conference on Big Data (Big Data)*, IEEE. pp. 4858–4863.
- Qian, N., 1999. On the momentum term in gradient descent learning algorithms. *Neural Networks* 12, 145–151.
- Rawla, P., Barsouk, A., 2019. Epidemiology of gastric cancer: global trends, risk factors and prevention. *Przegląd Gastroenterol* 14, 26–38.
- Redmon, J., Farhadi, A., 2018. YOLOv3: An incremental improvement. arXiv preprint arXiv:1804.02767 .
- Ren, S., He, K., Girshick, R., Sun, J., 2015. Faster R-CNN: Towards real-time object detection with region proposal networks. *Advances in neural information processing systems* 28.
- Roder, D.M., 2002. The epidemiology of gastric cancer. *Gastric cancer* 5, 5–11.
- Shibata, T., Teramoto, A., Yamada, H., Ohmiya, N., Saito, K., Fujita, H., 2020. Automated detection and segmentation of early gastric cancer from endoscopic images using mask r-cnn. *Applied Sciences* 10, 3842.
- Shrivastava, A., Gupta, A., Girshick, R., 2016. Training region-based object detectors with online hard example mining, in: *Proceedings of the IEEE Conference on Computer Vision and Pattern Recognition*, pp. 761–769.
- Smirnov, E., Melnikov, A., Oleinik, A., Ivanova, E., Kalinovskiy, I., Luckyanets, E., 2018. Hard example mining with auxiliary embeddings, in: *Proceedings of the IEEE Conference on Computer Vision and Pattern Recognition Workshops*, pp. 37–46.
- Tan, M., Le, Q., 2019. EfficientNet: Rethinking model scaling for convolutional neural networks, in: *International Conference on Machine Learning*, pp. 6105–6114.
- Tan, M., Pang, R., Le, Q.V., 2020. EfficientDet: Scalable and efficient object detection, in: *Proceedings of the IEEE/CVF conference on computer vision and pattern recognition*, pp. 10781–10790.
- Tang, Y.B., Yan, K., Tang, Y.X., Liu, J., Xiao, J., Summers, R.M., 2019. Uldor: a universal lesion detector for ct scans with pseudo masks and hard negative example mining, in: *2019 IEEE 16th International Symposium on Biomedical Imaging (ISBI 2019)*, IEEE. pp. 833–836.

- Togo, R., Yamamichi, N., Mabe, K., Takahashi, Y., Takeuchi, C., Kato, M., Sakamoto, N., Ishihara, K., Ogawa, T., Haseyama, M., 2019. Detection of gastritis by a deep convolutional neural network from double-contrast upper gastrointestinal barium X-ray radiography. *Journal of gastroenterology* 54, 321–329.
- Uemura, N., Okamoto, S., Yamamoto, S., Matsumura, N., Yamaguchi, S., Yamakido, M., Taniyama, K., Sasaki, N., Schlemper, R.J., 2001. Helicobacter pylori infection and the development of gastric cancer. *New England journal of medicine* 345, 784–789.
- Wang, C.Y., Bochkovskiy, A., Liao, H.Y.M., 2023. YOLOv7: Trainable bag-of-freebies sets new state-of-the-art for real-time object detectors, in: *Proceedings of the IEEE/CVF Conference on Computer Vision and Pattern Recognition*, pp. 7464–7475.
- Wu, L., Zhou, W., Wan, X., Zhang, J., Shen, L., Hu, S., Ding, Q., Mu, G., Yin, A., Huang, X., et al., 2019. A deep neural network improves endoscopic detection of early gastric cancer without blind spots. *Endoscopy* 51, 522–531.
- Zhang, K., Zhang, Z., Li, Z., Qiao, Y., 2016. Joint face detection and alignment using multitask cascaded convolutional networks. *IEEE Signal Processing Letters* 23, 1499–1503.
- Zhang, Z., Guo, Y., Lu, Y., Li, S., 2019. Detection of metastatic lymph nodules in gastric cancer using deep convolutional neural networks, in: *2019 IEEE/ASME International Conference on Advanced Intelligent Mechatronics (AIM)*, IEEE. pp. 942–947.

Graphical Abstract

Practical X-ray Gastric Cancer Screening Using Refined Stochastic Data Augmentation and Hard Boundary Box Training

Hideaki Okamoto, Takakiyo Nomura, Kazuhito Nabeshima, Jun Hashimoto, Hitoshi Iyatomi*



Highlights

Practical X-ray Gastric Cancer Screening Using Refined Stochastic Data Augmentation and Hard Boundary Box Training

Hideaki Okamoto, Takakiyo Nomura, Kazuhito Nabeshima, Jun Hashimoto, Hitoshi Iyatomi*

- We propose an unprecedented gastric cancer diagnostic support system for gastric X-rays, which can be taken by technicians and allow more people to be screened, rather than endoscopy, which is currently the mainstream but can only be performed by physicians. The system is based on a general deep learning-based object detection model and includes two novel technical proposals; a refined stochastic gastric image augmentation (R-sGAIA) and a hard boundary box learning (HBBT).
- A R-sGAIA is a probabilistic gastric fold region enhancement method to provide more learning patterns for cancer detection models.
- A HBBT is an efficient and versatile training method for common object detection models that allows the use of unannotated negative (i.e., healthy control) samples that cannot be used for training in conventional detection models. This reduces false positives and thus improves overall performance.
- The sensitivity of the proposed system for gastric cancer (90.2%) exceeds that of the expert (85.5%), while 42.5% of the detected candidate box regions show cancerous lesions, with a processing time of 0.51 seconds/image. The proposed system showed 5.9 points higher on the F1 score compared to methods using the same object detection model and state-of-the-art data augmentation. In short, the system quickly and efficiently shows the radiologist where to look, greatly reducing the radiologist's workload.

Practical X-ray Gastric Cancer Screening Using Refined Stochastic Data Augmentation and Hard Boundary Box Training

Hideaki Okamoto^a, Takakiyo Nomura^b, Kazuhito Nabeshima^b, Jun Hashimoto^b, Hitoshi Iyatomi^{*a}

^a*Department of Applied Informatics, Graduate School of Science and Engineering, Hosei University, 3-7-2*

Kajino, Koganei, 184-8584, Tokyo, Japan

^b*Department of Radiology, Tokai University School of Medicine, 143 Shimokasuya, Isehara, 259-1193, Kanagawa, Japan*

Abstract

Endoscopy is widely used to diagnose gastric cancer and has a high diagnostic performance, but because it must be performed by a physician, the number of people who can be diagnosed is limited. Gastric X-ray, on the other hand, can be performed by technicians and can screen a much larger number of patients than endoscopy, but its correct diagnosis requires experience. We propose an unprecedented and practical gastric cancer diagnosis support system for gastric X-ray images, which will enable more people to be screened. The system is based on a general deep learning-based object detection model and includes two novel technical proposals: refined probabilistic stomach image augmentation (R-sGAIA) and hard boundary box learning (HBBT). R-sGAIA is a probabilistic gastric fold region enhancement method that provides more learning patterns for cancer detection models. HBBT is an efficient training method for object detection models that allows the use of unannotated negative (i.e., healthy control) samples that cannot be used for training in conventional detection models, thereby improving model performance. The sensitivity (SE) of the proposed system for gastric cancer (90.2%) is higher than that of the expert (85.5%), and two out of five candidates detected box are cancerous, achieving a high precision while maintaining a high processing speed of 0.51 seconds/image. The proposed system showed 5.9 points higher on the F1 score compared to methods using the same object detection model and state-of-the-art data augmentation. In short, the system quickly and efficiently shows the radiologist where to look, greatly reducing the radiologist's workload.

Declarations of interest: none

Keywords: Gastric cancer, X-ray, screening, data augmentation, hard negative mining, computer-aided diagnosis

1. Introduction

Gastric cancer is the third most deadly cancer in the world with a poor prognosis, especially in the advanced stages (Rawla and Barsouk, 2019). However, early prognosis before metastasis can improve outcome; therefore, early detection and appropriate treatment are important. Gastric cancer is primarily diagnosed by endoscopy or radiography. Endoscopy reported a sensitivity (SE) of 95.4%, which is superior to other methods such as gastric radiography or X-ray at 85.5% (Hamashima et al., 2013). However, endoscopy can only be performed by a physician, and the time and cost involved limits

*Corresponding author

Email address: iyatomi@hosei.ac.jp (Hitoshi Iyatomi*)

the number of people who can be screened. Gastric X-ray, on the other hand, can be performed by radiographers and provides a large number of images, making it suitable for screening. This is a major advantage over endoscopic diagnosis. In Japan, a mass screening system was established, and in 2019, at least 3.87 million people underwent gastric X-ray for gastric cancer screening, with 183,000 people indicated as needing further testing, and 2,553 cases of gastric cancer were ultimately found. On the other hand, only 374,000 people underwent endoscopy for the same purpose and were confirmed (Matsuura, 2023). Although the effectiveness of endoscopy has led to a shift to this diagnostic method, the development of superior diagnostic support technology for gastric radiography would significantly contribute to the early detection and reduction of mortality from gastric cancer.

The gastric X-ray images obtained are later read by the doctor to diagnose the shape of the stomach and the atrophy of the mucosa membrane (Uemura et al., 2001; Roder, 2002; Correa et al., 2004). Another advantage of X-rays is that they can show minute irregularities that are indicative of stage IIc lesions (early stage tumor with a slight indentation) – slightly elevated component within the indentation that lies beneath the indentation. However, this is an area that requires a high level of reading skill, an area that many gastrointestinal angiographic studies are unable to diagnose. In other words, when performed by a skilled physician, the possibility of being able to assess the extent of cancerous invasion deep within the surface of an early stage cancer based on changes in the microscopic structure of the surface is high. Hence, the limitations of this diagnostic method are that it requires extensive physician experience in diagnosis and is particularly difficult to detect early-stage cancers, resulting in a cancer detection capacity that is inferior to that of endoscopy (Hibino et al., 2023). Therefore, there is a need to realize an automatic screening assistance system that can accurately and quickly detect gastric abnormalities from gastric X-ray images in clinical settings.

Healthy gastric folds are thin, smooth, and parallel; however, their thickness and size can be altered by gastric diseases, such as inflammation, infection, ulcers, and tumors, resulting in irregular bends, depressions, and tears in the lining mucosa (Correa et al., 2004). Most of the research on diagnostic support using gastric X-rays aimed at detecting gastritis, the stage before gastric cancer or the presence of *Helicobacter pylori* infection, which is believed to be the cause of gastric cancer (Cooper et al., 1990; Kita, 1992; Minemoto et al., 2010; Nagano and Matsuo, 2010; Abe et al., 2014; Ishihara et al., 2015, 2017; Togo et al., 2019; Kanai et al., 2019, 2020). Among these proposals, methods based on deep learning represented by convolutional neural networks (CNNs) have reported excellent results in the detection of gastritis. The main advantage of these deep learning techniques is that they can automatically capture efficient features for the target task, which is promising in this area where disease features are difficult to define. However, studies directly detecting gastric cancer from radiographs are limited despite of the significance of gastric cancer diagnosis in terms of life expectancy. This may be because gastric cancer is more difficult to diagnose, especially in the early stages, compared to gastritis, where the lesion often expands and develops to some degree. Reportedly, it is difficult to distinguish gastritis from gastric cancer even when using the latest machine learning techniques on endoscopic images where signs of the disease are easily visible (Horiuchi et al., 2020).

In the field of computer vision research, CNN-based object detection methods (e.g., Faster R-CNN (Ren et al., 2015), YOLOv3 (Redmon and Farhadi, 2018), EfficientDet (Tan et al., 2020), and YOLOv7 (Wang et al., 2023)), which can simultaneously detect and classify the location of multiple objects in images, have been proposed and widely used. Because these object detection methods can identify the regions involved, they have high explanatory power for the predicted results, as opposed to simply determining benign or malignant on an image-by-image basis. These features are extremely important in medical applications (Hirasawa et al., 2018; Li et al., 2018; Okamoto et al., 2019; Laddha et al., 2019; Zhang et al., 2019). In a study of gastric X-ray images, Laddha et al. (2019) used YOLOv3 to automatically detect gastric polyps, achieving a mean average precision of 0.916. On the other hand,

these object detection methods require annotation of lesion locations prior to training, which is extremely expensive. The aforementioned gastritis detection studies (Ishihara et al., 2017; Togo et al., 2019; Kanai et al., 2019, 2020) used a patch-based CNN that only needed to be annotated on an image-by-image basis to avoid high annotation costs while fully understanding the explanatory advantages provided by the object detection model. However, in gastric cancer, where diagnostic difficulties and outcomes are more severe, it is critical that physicians are able to interpret the results of diagnostic support systems.

With this motivation, we proposed a diagnostic support system that directly targets gastric cancer using X-ray images, which have rarely been studied, and provides high explanatory power for the results (Okamoto et al., 2019). Thanks to the proposed stochastic gastric image augmentation (sGAIA) based on medical knowledge, this system was able to represent candidate regions of gastric cancer in a boundary box with high accuracy. The recall (= SE) and precision of the detected bounding boxes were 92.3% and 32.4%, respectively, in an evaluation using images of patients different from the training set. This is about 7% higher recall than that achieved by doctors (85.5%), and the box-by-box evaluation confirmed that the ratio of true to false detections was 1:3, which is sufficient for practical use. The object detection model trained with the sGAIA has achieved a practical level of accuracy; however, further performance improvements are desirable.

Currently, widely used object detection methods have the disadvantage of not being able to explicitly use negative (i.e., healthy control) data for learning, in addition to the high cost of annotation. When such models are used for lesion detection, only images with lesions are used for training; control images without lesions cannot be used. There is much room for improvement here, which is one of the main themes of the work in this study. When dealing with medical images, data are expensive, and we believe that actively using healthy control images that do not contain lesions for training can improve the overall ability of the model to detect lesions. This is equivalent to reducing the cost of annotation to achieve the same performance.

In this study, we proposed a practical gastric cancer screening system. The system includes two new proposals: refined stochastic gastric image augmentation (R-sGAIA), which is an improvement of sGAIA (Okamoto et al., 2019), and hard boundary box training (HBBT, enables the learning of negative or healthy control images), which have not been previously explicitly utilized for training in object detection neural networks. To suppress the high-confidence false positives predicted by the object detector, HBBT registers each of these boxes as a “hard-sample” class and retrain the model until the predetermined convergence conditions are met. We investigated 4,608 gastric X-ray images obtained from 140 patients in a clinical setting and confirmed the practicality and effectiveness of the proposed system by evaluating gastric cancer detection performance with a patient-based cross-validation strategy.

The contributions of this study are as follows:

- We proposed an unprecedented gastric cancer diagnostic support system for gastric X-rays, which can be taken by technicians. As a result, this allows more people to be screened, rather than endoscopy, which is currently the mainstream but can only be performed by physicians. The system is based on a general deep learning-based object detection model and includes two novel technical proposals: R-sGAIA and HBBT.
- R-sGAIA is a probabilistic gastric fold region enhancement method used to provide more learning patterns for cancer detection models.
- HBBT is an efficient and versatile training method for common object detection models that allows the use of unannotated negative (i.e., healthy control) samples that otherwise cannot be used for training in conventional detection models. This reduces false positives and thus improves overall performance.

- The SE of the proposed system for gastric cancer (90.2%) exceeds that of the expert (85.5%), while 42.5% of the detected candidate box regions show cancerous lesions, with a processing time of 0.51 s/image. The proposed system showed 5.9 points higher on the F1 score compared to methods using the same object detection model and state-of-the-art data augmentation. In short, the system quickly and efficiently shows the radiologist where to look, greatly reducing the radiologist’s workload.

2. Related work

2.1. Diagnostic support using gastric X-ray images

In the 1990s, methods for effectively extracting the pattern of gastric folds by applying binarization as a preprocessing step and for estimating the gastric region based on the position of the barium reservoir were proposed (Cooper et al., 1990; Kita, 1992). In the 2010s, more empirical studies focused on gastric folds began to emerge (Minemoto et al., 2010; Nagano and Matsuo, 2010; Abe et al., 2014; Ishihara et al., 2015). Ishihara et al. (2015) calculated numerous statistical features (7,760 per case) for *H. pylori* infection, a major cause of gastric cancer, by focusing on post-infection mucosal patterns and gastric folds. Their support vector machine based on the data of 2,100 patients, 8 per person, yielded an SE of 89.5% and a specificity (SP) of 89.6%.

Recently, taking advantage of deep learning techniques, research has been conducted on the detection of gastritis using patch-based CNNs on gastric X-ray images (Ishihara et al., 2017; Togo et al., 2019; Kanai et al., 2019, 2020). Although these methods targeted gastritis, which is easier to diagnose than gastric cancer, they achieved high detection accuracy and were considered practical in diagnostic assistance. Kanai et al. (2020) used a patch-based CNN to detect *H. pylori*-associated chronic atrophic gastritis. They trained image patches of the inside and outside of the stomach and made a diagnosis by a majority vote of each estimated result in the stomach region. Manual annotation of regions of interest (ROIs) prior to training and self-learning to increase the number of training patches ultimately yielded a harmonic mean SE and SP of 95.5% for the test data of different patients.

While excellent screening results have been achieved for gastritis, the detection of more serious and difficult to diagnose gastric cancers has not been well studied. In the case of gastric cancer, it is also important to provide an explanation for the results. The proposed method is a significant improvement of our previous work, a gastric cancer detection system that can present explainable results (Okamoto et al., 2019), with two new technical proposals.

2.2. Diagnostic support research for endoscopic images

In recent years, many methods for analyzing narrow-band endoscopy images to assist in the diagnosis of gastric cancer using deep learning technology have been proposed (Kanayama et al., 2019; Wu et al., 2019; Horiuchi et al., 2020; Li et al., 2020; Gong et al., 2023).

Wu et al.’s (2019) classic VGG16 or ResNet-50 models achieved an SE of 94.0% and an SP of 91.0% based on 24,549 images for diagnosing early gastric cancer. Li et al.’s (2020) Inception-v3 model achieved an SE of 91.2% and SP of 90.6% based on 2,429 images of gastric magnification endoscopy with narrow-band imaging. Horiuchi et al. (2020) trained GoogLeNet with 1,499 images of gastric cancer and 1,078 images of gastritis and achieved an SE of 95.4%, an SP of 71.0%, and an area under the receiver operating characteristic (ROC) curve (AUC) of 0.852. Gong et al. (2023) developed a Convolution and Relative Self-Attention Parallel Network based on 3,576 endoscopic images taken from 205 patients. They reported achieving $F1 = 0.948$ in their experiments with a 7:3 split of training and test images. Although these methods produce excellent results, none of them have statements that clearly separate the training dataset from the patients for whom the images in the evaluation set were taken. In other

words, it is possible that the same patient images are mixed in the training and test data. In this case, the test data, which were very close to the training data, were evaluated, resulting in a score that was much higher than the original ability.

Kanayama et al. (2019) constructed a diagnostic support system using 129,692 gastrointestinal endoscopy images with sophisticated CNN-based networks, including one synthesizer network and two different types of discriminator networks. Furthermore, the images of the same patient were not divided into training and evaluation sets; that is, the performance were evaluated appropriately. They reported an average precision (AP) of 0.596 in cancer detection performance. Although the numerical performance of this method appears inferior, it is based on a newer and more sophisticated ML model than previously reported methods and is considered to represent a true diagnostic capability for this problem based on current machine learning techniques. They generated 20,000 high-resolution lesion images from 1,315 narrow-field-of-view images of the lesion using their own generative adversarial network (Goodfellow et al., 2014) and added these images to the training set. As a result, the AP reported an improvement in cancer detection performance to 0.632. Shibata et al. (2020) constructed and rigorously evaluated a diagnostic model using Mask R-CNN on 1,208 and 533 images each obtained from 42 healthy subjects and 93 unhealthy subjects (including gastric cancer), respectively. Their model achieved an SE of 96% for all tumor types, a false positive of 0.1/image, and $F1 = 0.71$ for gastric cancer. Ahmad et al. (2023) trained and evaluated a larger dataset than previous studies (27,200 training and 6,800 testing) with a unique improved method that added Squeeze and Excitation attention blocks to YOLO-v7 (Wang et al., 2023), achieving $F1 = 0.71$ (precision = 72%, recall = 69%). While we could not confirm if proper data partitioning was done, it is important to note that the number of images used for training and evaluation was sufficiently large compared to other studies. In addition, the study used more sophisticated methods, with results different from the previous studies (about 90% in F1 and higher) where substantial data leakage was considered to have occurred. Lastly, the results were comparable to other reports (Shibata et al., 2020) where the distinction was clearly split. It can be inferred that the data division was appropriate.

2.3. *Hard negative mining*

Hard sample or hard example mining, which improves model performance by explicitly retraining the model on error-prone or hard-to-identify data (hard samples), is widely used in machine learning (Felzenszwalb et al., 2009; Shrivastava et al., 2016). It is an effective method for counteracting the imbalance of each class and has been widely used, together with metric learning, for face or person detection from complex backgrounds (Zhang et al., 2016; Smirnov et al., 2018; Chen et al., 2020) and other applications.

In recent years, deep learning-based object detection models have also incorporated this strategy and reported many performance improvements by relearning misdetected bounding box regions, with results in the medical field (Li et al., 2019; Tang et al., 2019). However, such object detection models cannot use images that do not contain a single class of detection targets (such as background images or medical healthy control images) for training. This is because the error function to be minimized is defined based on the position and size of the bounding box of each detection target. Existing hard sample mining methods have been applied to data with at least one annotation box of the class to be detected and have used overdetected or undetected regions or image patches as hard samples. Our HBBT is a hard sample mining or hard negative mining; that is, it retrains regions of false positives but differs significantly in that it allows the use of healthy control cases, which could not be used to train object detection models, for training. This is a particularly important contribution in the medical field, where the cost of positive samples is high.

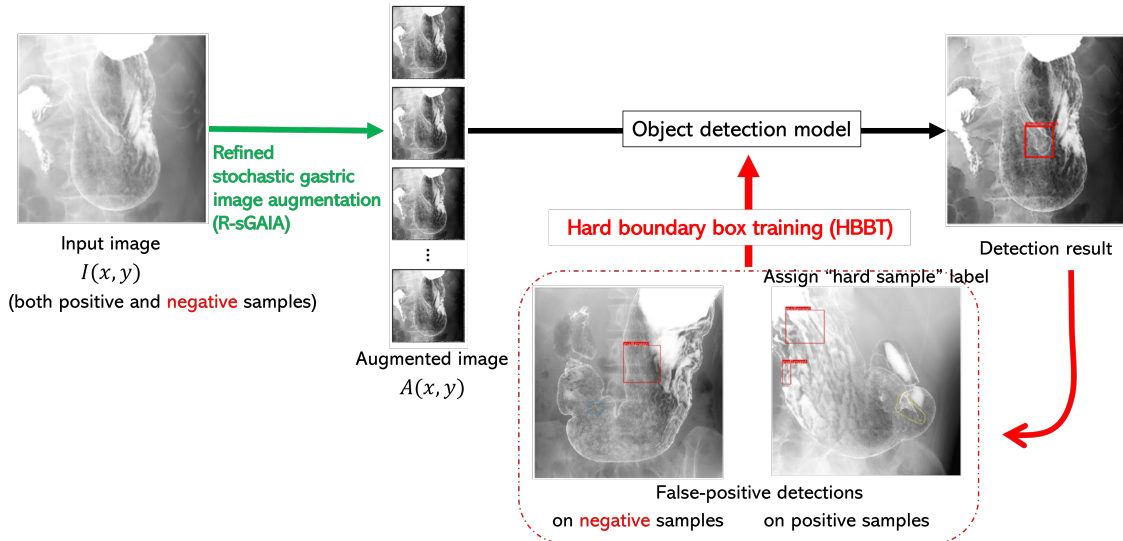


Figure 1: Overview of the proposed gastric cancer screening system.

3. Practical gastric cancer screening system

This study proposed a practical gastric cancer screening system using gastric X-ray images. The system displayed suspected cancerous sites with bounding boxes so physicians can confirm the validity of the estimation. The two technical proposals in this study significantly improved the performance of the system and achieved practical accuracy. The overall structure of the proposed system is shown in Figure 1. This study was approved by the Institutional Review Board of Tokai University Hospital (No. 20R-033, date of approval: June 12, 2020). The main technical proposals were (1) R-sGAIA to effectively detect gastric fold regions and (2) HBBT to avoid false positives by assigning “hard-sample” classes to the bounding box regions where false positives are detected and iteratively learning them. The object detection model used is EfficientDet (Tan et al., 2020), which uses EfficientNet (Tan and Le, 2019), a CNN with reported excellent performance, as its backbone, but the choice of the model used was arbitrary. The input was $2,048 \times 2,048$ pixels, and the output was a bounding box surrounding the presumed cancerous region in the image and its confidence score.

3.1. R-sGAIA

The proposed R-sGAIA is a refined version of our previous proposal, sGAIA (Okamoto et al., 2019). The proposed R-sGAIA and sGAIA are probabilistic online data augmentation methods that can generate various images highlighting gastric folds in X-ray images based on medical knowledge to detect inflammation on the gastric mucosal surface. The former sGAIA improved the detection of gastric cancer by 6.9% in terms of the F1-score (recall 92.3%, precision 32.4%) on a Faster R-CNN model with ResNet-101 as the backbone, validating its practical screening performance. However, in the sGAIA, the emphasis probability of each pixel $p(x, y)$, which is important for an effective enhancement, was subjectively determined as a discrete value based on the results of preliminary experiments. In the proposed R-sGAIA, $p(x, y)$ becomes a flexible continuous function based on only two hyperparameters.

A schematic of the proposed R-sGAIA process is shown in Figure 2. Like sGAIA, R-sGAIA consists of the following four steps, where only step 2 is different.

- (Step 1) Calculation of edge strength $E(x, y)$

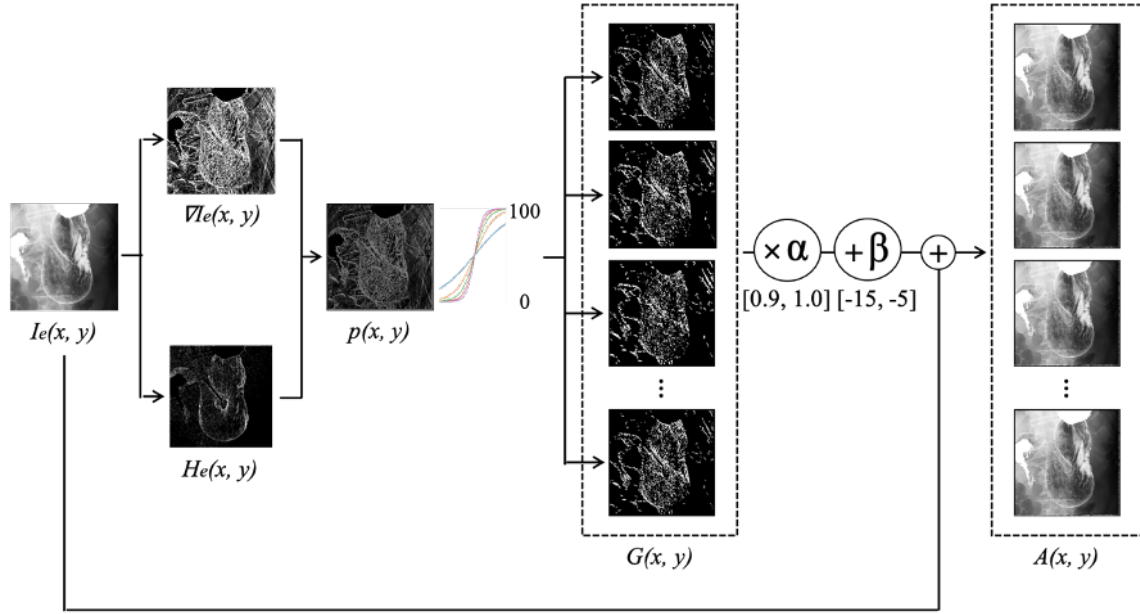


Figure 2: Overview of refined stochastic gastric image augmentation (R-sGAIA).

First, a contrast-enhanced image $I_e(x, y)$ is generated from the original gastric X-ray image $I(x, y)$ using histogram equalization. Then, its gradient and high-frequency components, $\nabla I_e(x, y)$, and $H_e(x, y)$, are obtained using general image processing techniques such as Canny edge detection filter and Butterworth high-pass filter, respectively. Each of them is normalized to $[0, 1]$, and the normalized edge strength $E(x, y)$ is calculated as follows:

$$E(x, y) = (\overline{\nabla I_e(x, y)} + \overline{H_e(x, y)})/2, \quad (1)$$

where $\overline{v(x, y)}$ is the linearly normalized value of $v(x, y)$ to $[0, 1]$.

- (Step 2) Calculation of the probability of a gastric fold region $p(x, y)$

The area of the edge of the gastric folds that is subject to augmentation is determined for each pixel as its probability $p(x, y)$. The proposed R-sGAIA differs from sGAIA in this step. In R-sGAIA, the edge intensity $e = E(x, y)$ of each pixel is used to obtain a probability map $p(x, y)$ of the gastric folds and edges using probabilities based on the sigmoid function defined below.

$$\begin{aligned} p(x, y) &= p(e) = p(E(x, y)) \\ &= \frac{1}{1 + \exp(-\gamma(E(x, y) + \theta))}. \end{aligned} \quad (2)$$

The parameters γ and θ are hyperparameters, respectively, defining the slope of the sigmoid function and adjusting the probability of running the augmentation of $E(x, y)$ to be 50%. They are determined based on the diagnostic performance of the validation data, as described below. Figure 3 compares the enhancement selection probability $p(e = E(x, y))$ based on the feature intensity e for R-sGAIA and sGAIA. Note that, in sGAIA, the probability $p(e)$ is subjectively determined based on preliminary experiments, as described above.

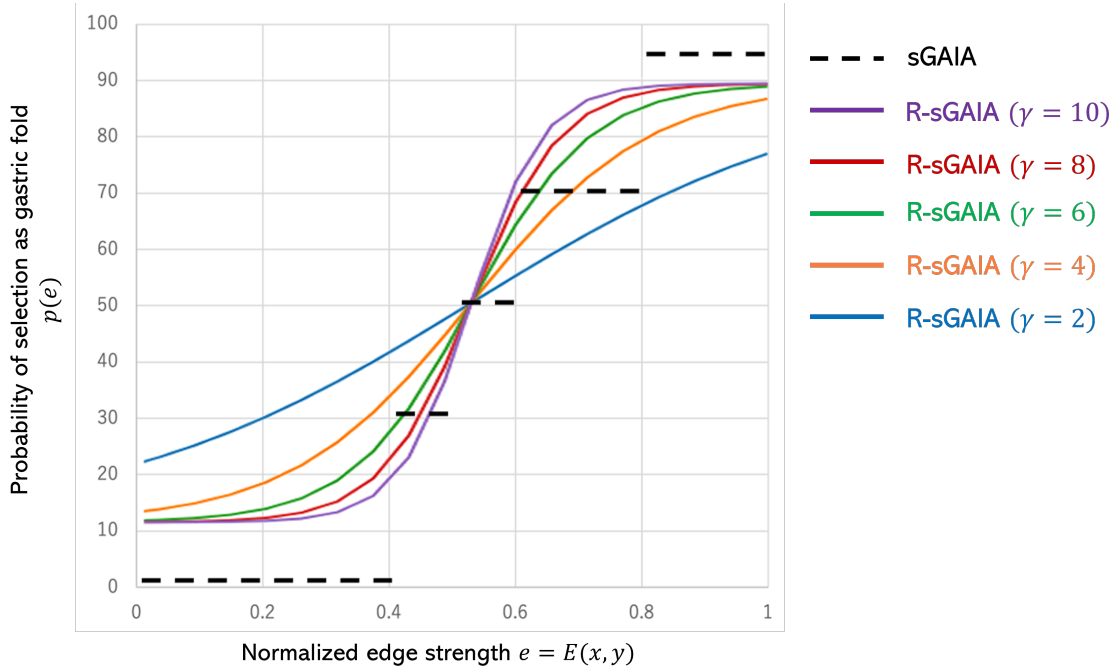


Figure 3: Probability of being detected as a gastric fold edge to be highlighted.

- (Step 3) Determination of gastric fold edge region $G(x, y)$

According to the probability map $P(x, y)$, a binary mask $G(x, y)$ of the gastric fold regions to be enhanced is determined by pixel-by-pixel sampling. Since this result is noisy, a morphological open operation is performed to remove many small isolated regions. $G(x, y)$ is created in such a way that a different mask is generated for each trial. This is the key to generating enhanced images of different gastric folds.

- (Step 4) Generation of enhanced gastric fold images $A(x, y)$

Finally, an enhanced gastric fold edge image $A(x, y)$ is obtained as follows:

$$A(x, y) = I_e(x, y) + \alpha G(x, y) + \beta. \quad (3)$$

Here, α and β are augmented parameters. The value of α ranges from 0.9 to 1.0 and that of β ranges from -15 to -5 , and they are chosen randomly for each processing. Based on this, the proposed R-sGAIA probabilistically enhances the location and intensity of the gastric fold region each time. Thus, it produces a different enhanced gastric image for each trial and is highly compatible with the online data augmentation in deep neural network training. Another significant advantage of the proposed R-sGAIA is that it does not require any additional runtime. We used this R-sGAIA for online augmentation of a machine learning model (i.e., EfficientDet-D7) used for cancer region detection.

3.2. HBBT

The diagnostic support system for gastric X-ray images is a one-class detection problem that targets only positive (i.e., malignant) regions. However, our task has many regions with similar image features, making them difficult to discriminate even for experts. Given a large number of training images, the recently developed deep learning-based object detection algorithms can achieve the desired detection

performance for the task, but this is difficult in situations where the labeled supervisory data is limited. The images in Figure 4 are typical false positives indicated by experts in experiments conducted using a vanilla detection model (i.e., EfficientDet-D7 without the proposed HBBT). The results show that most of these false positives fall broadly into the five categories shown in examples (b)–(f) in Figure 4. However, it is difficult to clearly define and control these features in advance. Specifically, in a fine-grained task like our current goal, it is very important to reduce such hard negatives that have high image similarity but are not the target.

One promising countermeasure to this problem is hard sample mining, of which hard negative mining, which aims to reduce over-detection, is consistent with this goal and has been extensively studied as mentioned above. However, the training of hard negative mining applied to object detection models is aimed at reducing false positives (hard negatives) outside the target region in the training image, and the data that can be used for training are subject to the constraints of the object detection model. In other words, the training data are only images with some object detection annotation label, unless a framework such as semi-supervised learning is used.

In fact, as mentioned earlier, the biggest room for improvement in object detection models is the active use of negative samples, i.e., healthy controls. Conventional object detection algorithms based on deep learning only use images in which there is an object to be detected, and control cases without an object to be detected cannot be included in the training. This is a very important limitation. Therefore, for more effective training of object detection models, we propose HBBT, a very simple and effective method for suppressing false positives, referring to the concept of hard negative mining. In general, training negative samples, which are more prone to false positives among the training data, is effective in constructing detectors with few false positives. In HBBT, as shown in Figure 1, the false-positive boundary boxes detected by the model are called hard boundary boxes and are given hard-sample labels to train the model as a two-class detection problem. This newly added hard-sample class label is treated as a negative example. Training is repeated until an optimal F1-score is obtained from the validation data. The important point here is that not only positive data (e.g., with cancerous regions), which can be used for normal training, but also negative (i.e., healthy, control) data, which are generally available in large quantities, can be used to detect hard boundary boxes, i.e., can be used for training.

4. Experiments

4.1. Datasets

The image set used in this study consisted of 4,724 gastric X-ray images (1,117 images with 1,504 lesion annotations by radiologists and 3,607 images without lesions) from 145 patients in clinical settings provided by the Tokai University School of Medicine, Japan. A total of 116 images from five randomly selected patients (49 of them with 49 annotated boxes) were used as validation data to determine the hyperparameters and the decision to terminate HBBT, and the remaining 4,608 images from 140 patients were used to train and evaluate the proposed system.

Each image was in 8-bit grayscale and had a resolution of $2,048 \times 2,048$ pixels. Based on each expert annotation of the gastric cancer locations, the smallest rectangle surrounding each location was defined as a bounding box to be detected. A patient-based five-group cross-validation was used for training and evaluation. Precision, recall, and F1-score were used as the performance indicators of this system. The system provided candidate lesion bounding boxes and their associated confidence scores were above a predefined detection threshold ξ .

4.2. Details of the detection model

We used EfficientDet-D7 (Tan et al., 2020) as a gastric cancer detection model with an input resolution of $1,536 \times 1,536$ pixels. One difference from the original image size was the margin for random

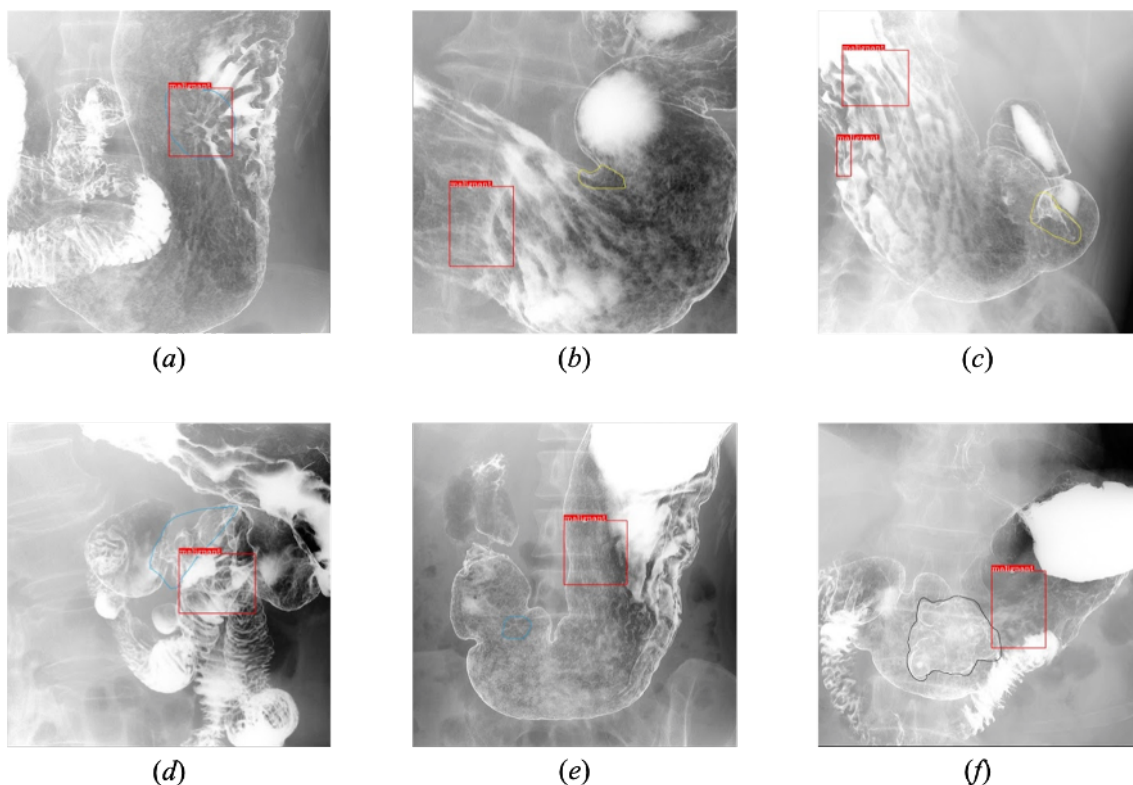


Figure 4: Positive example and five typical false positives provided by experts.

(a) Positive example. (b) The area overlapping the osteophytes and spinous processes of the vertebral body. (c) Area where folds are gathered due to lack of air in the stomach. (d) Area where the duodenal Kerckring’s folds overlap with the stomach. (e) Areas where the mucosal surface of the stomach is irregular due to chronic gastritis. (f) Areas of advanced cancer that appear as wall changes rather than masses.

cropping performed during training. The entire networks are trained end-to-end and, as a result, can simultaneously estimate the detection target at any location and size in the input image and its content (i.e., "cancer"). See the original paper for details on the model. The learning rate was 0.001, the batch size was 32, and the number of trainings was 100. The optimization method used was momentum SGD (Qian, 1999), and the exponential decay rate of the first-order moment was set to 0.9. To construct the proposed gastric cancer detection system, the proposed R-sGAIA was applied as an online augmentation to train this model, and healthy control images without cancer lesions, which could not be used in general object detection models, were also used for training by using HBBT.

4.3. Experimental conditions

4.3.1. Determination of hyperparameters in R-sGAIA

In this section, we describe the hyperparameters θ and γ of the proposed R-sGAIA. θ is a hyperparameter that determines the edge strength $E(x, y)$ for which the probability of being considered a gastric fold is 50% in the sigmoid function $p(e = E(x, y))$ and was determined to be 0.55 based on the distribution of validation results. For γ , which characterizes the slope of $p(e)$, we selected $\gamma = 4$ from 2, 4, 6, 8, and 10 (Table 1) from the detection performance on validation images.

Table 1: Detection performance in validation images for determining hyperparameter γ .

γ	Precision (%)	Recall (%)	F1-score
2	35.7	89.6	0.511
4	39.6	91.7	0.553
6	31.2	91.7	0.466
8	32.8	89.6	0.480
10	30.3	89.6	0.453

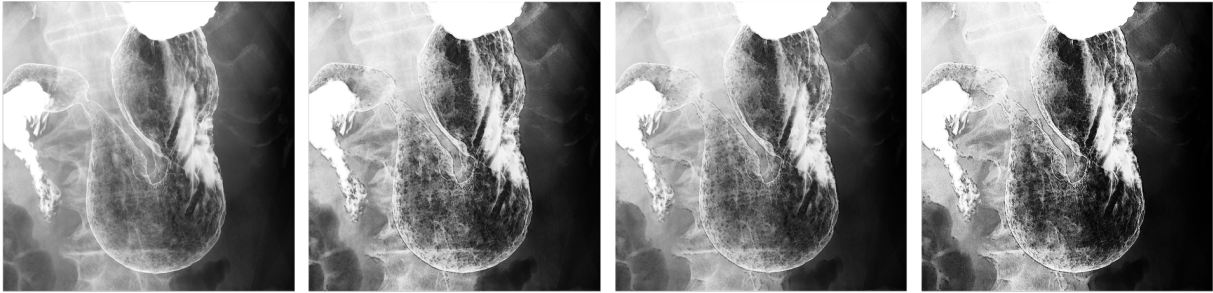


Figure 5: Example of augmented images (leftmost: original, others: enhanced images with R-sGAIA).

4.3.2. Detection of suspicious cancerous regions

To confirm the effectiveness of the proposed system with R-sGAIA and HBBT, we conducted comparative experiments using the following combinations of conditions. Since there is no directly comparable literature on gastric cancer detection, we implemented Laddha et al.’s (2019) method based on YOLO-v3 and compared the performance on our task.

- Model selection

We selected two deep learning-based object detection models for this task: ResNet-101+Faster R-CNN (model 1) and EfficientDet-D7 (model 2). The first model has been widely used in the literature, including sGAIA. The second model is one of the advanced object detection models used in many studies, although newer models are currently being proposed. RandAugment (Cubuk et al., 2020), one of the state-of-the-art online augmentation methods, was applied to these models and used as the baseline for each model (i.e., baseline models 1 and 2, respectively). Here, color augmentation was omitted because this task deals with grayscale images. Based on the detection performance of the validation dataset, 4 of the 13 augment types were selected with an intensity level of 3 (i.e., $M = 4$ and $N = 3$ according to their notation).

- Comprehensive evaluation of the proposals

We compared the performance of each model with and without the proposed technique. Regarding data augmentation, we chose either RandAugment, conventional sGAIA (+sGAIA), or the proposed R-sGAIA (+R-sGAIA). Regarding the proposed HBBT, this was annotated as use (+HBBT) or not.

5. Results

Figure 5 shows an example of the augmented image obtained with the proposed R-sGAIA for the leftmost original image. Figure 6 shows an example of the comparison of cancer detection on the

Table 2: Comparison of the detectability of gastric cancer sites.

	Augmentation			HBBT	Precision	Recall	F1-score
	RandAug [†]	sGAIA [‡]	R-sGAIA				
Laddha et al. (2019)*					26.5	89.7	0.409
Model 1 (Faster R-CNN on ResNet101)							
+ RandAugment (baseline model 1)	✓				28.4	90.1	0.432
+ sGAIA		✓			33.8	90.4	0.492
+ R-sGAIA			✓		36.4	90.2	0.519
+ R-sGAIA + HBBT (proposed)			✓	✓	38.7	90.1	0.541
Model 2 (EfficientDet-D7)							
+ RandAugment (baseline model 2)	✓				36.4	90.5	0.519
+ sGAIA		✓			37.9	90.1	0.534
+ R-sGAIA			✓		39.2	90.2	0.546
+ HBBT	✓			✓	39.4	89.9	0.548
+ R-sGAIA + HBBT (proposed)			✓	✓	42.5	90.2	0.578

* originally used for gastric polyp detection with YOLOv3 (Redmon and Farhadi, 2018).

[†] RandAugment (Cubuk et al., 2020) with $M = 4$ and $N = 3$.

[‡] sGAIA (Okamoto et al., 2019).

EfficientDet-D7 network (baseline model 2) with and without the proposed R-sGAIA and HBBT. Here are the input images (a), the detection results with RandAugment (b), and those with the proposed R-sGAIA+HBBT (c). The proposed system (c) could accurately detect the gastric cancer region without being affected by the unevenness of the mucosa, and small areas as shown in the top and middle rows, respectively. In contrast, as shown in the bottom row, the result almost covers the ROI but is misaligned; therefore, we evaluated it as a false-positive.

The detection performance of gastric cancer regions from gastric X-ray images is summarized in Table 2. The object detection model detects regions where the probability (i.e., the confidence score) of belonging to the class of interest exceeds a predefined detection threshold of the bounding box ξ as locations containing objects of that class. HBBT assigns new negative labels to the over-detected regions that exceed the threshold ξ and retrains the model. Therefore, to draw an ROC curve for evaluation, the model must be trained every time ξ is changed, which is expensive. In this experiment, therefore, the detection threshold ξ was determined such that the SE (= recall) of detecting gastric cancer was about 90%, which was higher than the doctor’s 85.5%. At this detection threshold, HBBT improves precision by 2.3 points in Faster R-CNN (baseline model 1) and 3.3 points in EfficientDet-D7 (baseline model 2). Our system using the proposed techniques, R-sGAIA and HBBT, achieved a recall of 90.2%, a precision of 42.5%, and an F1-score of 0.578 (Table 2).

The combination of the proposed R-sGAIA and HBBT showed a significant improvement over RandAugment, one of the most advanced data augmentations, in the detection of gastric cancer using the general object detection model. Specifically, the improvement was 10.3 points and 6.1 points in precision, and 10.9 points and 5.9 points in F1 scores for Faster R-CNN (model 1) and EfficientDet-D7 (model 2), respectively.

The processing time required to process one X-ray image is approximately 0.51 s, thus making the proposed system a suitable practical screening system for gastric X-ray images.

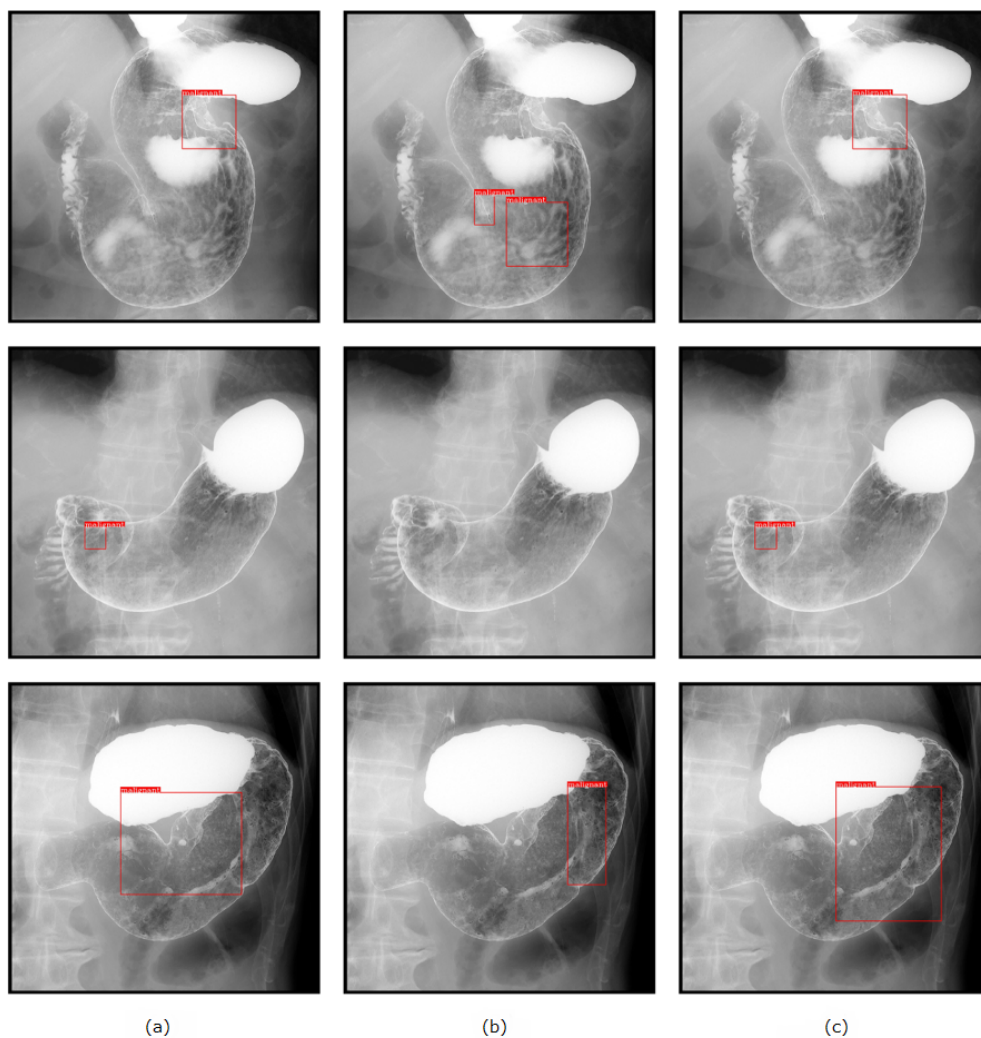


Figure 6: Example of cancer detection on EfficientDet-D7 networks: (a) ground-truth region, (b) results obtained with RandAugment (baseline model 2), and (c) those with R-sGAIA+HBBT (proposed). The proposed R-sGAIA+HBBT led to the accurate detection for the top and middle examples, whereas for the bottom result, although it showed some improvement, the detection was inaccurate.

6. Discussion

The cancer detection performance of the proposed system in this study was significantly better than those achieved using the baseline methods, including RandAugment (a state-of-the-art general data augmentation strategy), the existing methods such as sGAIA Okamoto et al. (2019), and those proposed by (Laddha et al., 2019). In addition, its cancer detection capability was higher than that of the physician’s reading ($\sim 85.5\%$). In terms of percentage, more than 2 out of 5 detection results presented were cancer. From the standpoint of a physician using the system, this means that the system can provide a higher diagnostic yield than a conventional physician’s reading simply by checking only the areas surrounded by the few bounding boxes presented by the system in a gastric X-ray image. In other words, the system is practically effective for on-site medical examinations and can significantly reduce the burden on physicians.

6.1. R-sGAIA

The proposed R-sGAIA can probabilistically highlight the gastric folds on a pixel-by-pixel basis based on the medical findings, as shown in Figure 5. In this study, we found that the proposed R-sGAIA achieved 6.0 points and 2.7 points better performance in terms of the F1-score than RandAugment on baseline models 1 and 2, respectively. This confirms the importance of probabilistic augmentation based on medical knowledge. In baseline model 2, R-sGAIA further improved the F1-score by 1.2 points over the previous sGAIA in a stand-alone comparison. This may be because R-sGAIA used validation data to determine $p(e)$ as a continuous function and was thus able to generate many types of enhancement images that better enhanced the gastric folds than sGAIA, which used a subjectively fixed value. The fact that the function of $p(e)$ with respect to the edge strength $e = E(x, y)$ was approximately between 0.1 and 0.9 is believed to have contributed to the performance improvement by allowing more stochastic variation than sGAIA in the very strong and weak edge strength regions, i.e., by contributing to the diversity of the generated images.

6.2. HBBT

All recent state-of-the-art box object detection models (e.g., YOLOv7 (Wang et al., 2023)) are trained in such a way that the difference between the boxes specified in the training data and the currently detected boxes simultaneously becomes smaller in both their classes (i.e., contents) and locations. In other words, the sum of the class error and position error for each box is the error of the model, and training is performed to minimize them.

The proposed HBBT is a new and effective strategy that also allows learning from healthy control images, which cannot be used to train conventional object detection models, and retrains over-detected boxes by assigning them a unique “hard-sample” class label to suppress future detections. The HBBT strategy of labeling error-prone regions (i.e., hard samples) with the hard sample class corresponds to increasing the class error of the model for these regions and retraining it to reduce false positives. In other words, the HBBT learning algorithm does not focus on the type of object detection model, because from a machine learning perspective, it is rather a strategy to reduce generic errors in these models. Furthermore, the proposed HBBT actively uses negative samples, in this case images of healthy controls, which cannot be used for training by conventional object detection models.

Although the HBBT is a very simple method that recursively learns to eliminate false positives detected on images, including control images, it alone improves precision by 2.3 points and 3.3 points and F1 score by 4.9 points and 2.9 points on baseline models 1 and 2, respectively. The HBBT is a general-purpose learning method that can be combined with any object detection algorithm, not just gastric cancer detection as in this case. Since the final model detection is determined by the bounding box confidence threshold, HBBT reduces not only the number of false positives but also the number of false negatives (middle case in Figure 6).

6.3. For practical screening

In this diagnostic support system, the response to the diversity in size and shape of the tumor area to be detected depends on the detectability of the object detection model used, and the range of object sizes that can be detected is determined by the hyperparameters (e.g., anchor size and aspect ratio). In the task of cancer detection from gastric X-ray images, the general settings of the object recognition model are not problematic because the images are taken in a way that the size of the tumor in the image does not appear too small to enable the physician to diagnose it visually. However, when dealing with extremely small tumors, it is necessary to set hyperparameters that take their size into account.

Since R-sGAIA is an online data augmentation method and HBBT is a training method, they do not affect the execution time of the inspection. The processing time of 0.5 s per image under current

conditions is considered sufficiently practical, and further improvement of the detection model is expected to increase the speed in the future.

The detection of a gastric cancer region from X-ray images is inherently difficult, not only for automatic diagnostic systems but also for experts. Despite these difficulties, our two technological proposals, R-sGAIA and HBBT, have significantly improved the detection performance of gastric cancer and achieved a performance and speed that can actually be used by physicians as a diagnostic aid. Our diagnostic support system will make a concrete contribution to solving the problem of gastric radiography, which has been considered easy to acquire images but difficult to diagnose. In the future, we aim to examine the results more closely with the help of experts to further improve the system further.

6.4. Comparison with automated diagnostic support methods for other modalities

Many diagnostic support studies have been conducted on endoscopy, which is the most commonly used method for diagnosing gastric cancer. However, as mentioned above, most of these studies did not or failed to properly separate the training data from the evaluation data, i.e., the training data is effectively leaked, and reported inappropriately high diagnostic performance. Recent studies with proper separation of these data using more sophisticated machine learning methods Shibata et al. (2020); Ahmad et al. (2023) reported a detection performance for gastric cancer of about 0.7 on an image-based F1 score, which is considered the currently feasible diagnostic accuracy.

Owing to its noninvasiveness and whole-body imaging, X-ray computed tomography (CT) is widely used not only for gastric cancer but also for detecting other organs and diseases. Diagnostic studies of gastric cancer for this modality generally use classical CT radiomics as the analytical factor, including the necessary pre-treatment, and depending on the stage, its diagnostic performance is approximately AUC 0.7 – 0.8 Meng et al. (2020); Huang et al. (2022). The application of deep learning technology is mainly for patient prognosis prediction and segmentation of tumor areas, rather than diagnosis of cancer itself. Hao et al. (2022) showed that radiomic features and features extracted by machine learning techniques (i.e., low-dimensional representations) are effective in predicting the prognosis of patients with gastric cancer. It is expected that these machine learning techniques will be used in the future.

The diagnostic performance of these automated diagnostic support methods appears to be lower than the 95% SE of physicians for gastric cancer; however, this is patient-based, and direct comparisons cannot be made. When automated diagnostic methods are introduced in clinical practice, the actual performance will be much closer to the current SE of physicians because multiple outputs can be integrated to make a decision, and this will be a great aid to physician diagnosis. Although our $F1 = 0.578$ for the diagnostic performance of gastric X-ray is numerically lower than those of other modalities, it is a box-based evaluation. In addition, since the physician makes a diagnosis by referring to multiple images in a gastric X-ray examination, the ability to indicate the ROI for each image makes our method very useful. Our method is also significant because it is the first time that a gastric X-ray image has been used to aid in the diagnosis of gastric cancer.

6.5. Limitations of the study

In recent years, it has become known that medical images such as MR images contain features unique to each facility due to differences in imaging equipment, protocols, geometry, etc., and that these differences (so-called domain differences) affect the results when machine learning tasks such as classification are applied as is. The gastric X-ray images used in this study were taken only at medical facilities affiliated with Tokai University. The effect of this domain difference may be observed in the analysis of gastric X-ray images taken at different facilities, but this has not been verified.

7. Conclusions

In this paper, we have proposed an unprecedented, accurate, and fast gastric cancer screening system from gastric X-ray images based on two technical proposals: (1) R-sGAIA and (2) HBBT. The cancer detection performance of the proposed system (R-sGAIA + HBBT on EfficientDet-D7 network), the system achieves a SE of 90.2%, which is higher than physicians (85.5%) with a processing time of approximately 0.5 seconds per image. At this time, 42.5% of the presented candidate box regions contain cancer. In other words, our system is practical in that it can very well limit the areas that physicians need to check. This performance is 5.9 points higher in F1 score than the same network using RandAugment, a state-of-the-art data augmentation method. The diagnosis of gastric cancer using gastric X-ray is a difficult task that requires long experience. We hope that our proposal will help in the diagnosis, leading to early detection and a reduction in the number of deaths in the near future.

Acknowledgments

This research was supported in part by the Ministry of Education, Science, Sports and Culture of Japan (JSPS KAKENHI), Grant-in-Aid for Scientific Research (C), 22K07728, 2022–2024. No financial support was received that would have influenced the results of this study.

H. Okamoto was responsible for the practical system development of the study and the writing of the paper; T. Nomura, K. Nabeshima, and J. Hashimoto provided medical guidance, data collection, diagnosis, and other insights; and J. Hashimoto and H. Iyatomi were responsible for the study design, overall management, and writing of the paper.

References

- Abe, K., Nakagawa, H., Minami, M., Tian, H., 2014. Features for discriminating normal cases in mass screening for gastric cancer with double contrast X-ray images of stomach. *Journal of Biomedical Engineering and Medical Imaging* 1.
- Ahmad, S., Kim, J.S., Park, D.K., Whangbo, T., 2023. Automated detection of gastric lesions in endoscopic images by leveraging attention-based yolov7. *IEEE Access* .
- Chen, K., Chen, Y., Han, C., Sang, N., Gao, C., 2020. Hard sample mining makes person re-identification more efficient and accurate. *Neurocomputing* 382, 259–267.
- Cooper, J., Khan, G., Taylor, G., Tickle, I., Blundell, T., 1990. X-ray analyses of aspartic proteinases: II. Three-dimensional structure of the hexagonal crystal form of porcine pepsin at 2.3 Å resolution. *Journal of Molecular Biology* 214, 199–222.
- Correa, P., Piazzuelo, M.B., Camargo, M.C., 2004. The future of gastric cancer prevention. *Gastric Cancer* 7, 9–16.
- Cubuk, E.D., Zoph, B., Shlens, J., Le, Q.V., 2020. RandAugment: Practical automated data augmentation with a reduced search space, in: *Proceedings of the IEEE/CVF Conference on Computer Vision and Pattern Recognition Workshops*, pp. 702–703.
- Felzenszwalb, P.F., Girshick, R.B., McAllester, D., Ramanan, D., 2009. Object detection with discriminatively trained part-based models. *IEEE Transactions on Pattern Analysis and Machine Intelligence* 32, 1627–1645.

- Gong, D., Yan, L., Gu, B., Zhang, R., Mao, X., He, S., 2023. A computer-assisted diagnosis system for the detection of chronic gastritis in endoscopic images using a novel convolution and relative self-attention parallel network. *IEEE Access* 11, 116990–117003.
- Goodfellow, I., Pouget-Abadie, J., Mirza, M., Xu, B., Warde-Farley, D., Ozair, S., Courville, A., Bengio, Y., 2014. Generative adversarial nets. *Advances in Neural Information Processing Systems* 27.
- Hamashima, C., Okamoto, M., Shabana, M., Osaki, Y., Kishimoto, T., 2013. Sensitivity of endoscopic screening for gastric cancer by the incidence method. *International Journal of Cancer* 133, 653–659.
- Hao, D., Li, Q., Feng, Q.X., Qi, L., Liu, X.S., Arefan, D., Zhang, Y.D., Wu, S., 2022. Identifying prognostic markers from clinical, radiomics, and deep learning imaging features for gastric cancer survival prediction. *Frontiers in oncology* 11, 725889.
- Hibino, M., Hamashima, C., Iwata, M., Terasawa, T., 2023. Radiographic and endoscopic screening to reduce gastric cancer mortality: a systematic review and meta-analysis. *The Lancet Regional Health–Western Pacific* 35, 100741.
- Hirasawa, T., Aoyama, K., Tanimoto, T., Ishihara, S., Shichijo, S., Ozawa, T., Ohnishi, T., Fujishiro, M., Matsuo, K., Fujisaki, J., et al., 2018. Application of artificial intelligence using a convolutional neural network for detecting gastric cancer in endoscopic images. *Gastric Cancer* 21, 653–660.
- Horiuchi, Y., Aoyama, K., Tokai, Y., Hirasawa, T., Yoshimizu, S., Ishiyama, A., Yoshio, T., Tsuchida, T., Fujisaki, J., Tada, T., 2020. Convolutional neural network for differentiating gastric cancer from gastritis using magnified endoscopy with narrow band imaging. *Digestive Diseases and Sciences* 65, 1355–1363.
- Huang, H., Xu, F., Chen, Q., Hu, H., Qi, F., Zhao, J., 2022. The value of CT-based radiomics nomogram in differential diagnosis of different histological types of gastric cancer. *Physical and Engineering Sciences in Medicine* 45, 1063–1071.
- Ishihara, K., Ogawa, T., Haseyama, M., 2015. Helicobacter pylori infection detection from multiple X-ray images based on combination use of support vector machine and multiple kernel learning, in: 2015 IEEE International Conference on Image Processing (ICIP), IEEE. pp. 4728–4732.
- Ishihara, K., Ogawa, T., Haseyama, M., 2017. Detection of gastric cancer risk from X-ray images via patch-based convolutional neural network, in: 2017 IEEE International Conference on Image Processing (ICIP), IEEE. pp. 2055–2059.
- Kanai, M., Togo, R., Ogawa, T., Haseyama, M., 2019. Gastritis detection from gastric X-ray images via fine-tuning of patch-based deep convolutional neural network, in: 2019 IEEE International Conference on Image Processing (ICIP), IEEE. pp. 1371–1375.
- Kanai, M., Togo, R., Ogawa, T., Haseyama, M., 2020. Chronic atrophic gastritis detection with a convolutional neural network considering stomach regions. *World Journal of Gastroenterology* 26, 3650.
- Kanayama, T., Kurose, Y., Tanaka, K., Aida, K., Satoh, S., Kitsuregawa, M., Harada, T., 2019. Gastric cancer detection from endoscopic images using synthesis by GAN, in: *Medical Image Computing and Computer Assisted Intervention–MICCAI 2019: 22nd International Conference, Shenzhen, China, October 13–17, 2019, Proceedings, Part V* 22, Springer. pp. 530–538.

- Kita, Y., 1992. Model-driven contour extraction for physically deformed objects-application to analysis of stomach X-ray images, in: 1992 11th IAPR International Conference on Pattern Recognition, IEEE Computer Society. pp. 280–284.
- Laddha, M., Jindal, S., Wojciechowski, J., 2019. Gastric polyp detection using deep convolutional neural network, in: Proceedings of the 2019 4th International Conference on Biomedical Imaging, Signal Processing, pp. 55–59.
- Li, L., Chen, Y., Shen, Z., Zhang, X., Sang, J., Ding, Y., Yang, X., Li, J., Chen, M., Jin, C., et al., 2020. Convolutional neural network for the diagnosis of early gastric cancer based on magnifying narrow band imaging. *Gastric Cancer* 23, 126–132.
- Li, M., Wu, L., Wiliem, A., Zhao, K., Zhang, T., Lovell, B., 2019. Deep instance-level hard negative mining model for histopathology images, in: Medical Image Computing and Computer Assisted Intervention–MICCAI 2019: 22nd International Conference, Shenzhen, China, October 13–17, 2019, Proceedings, Part I 22, Springer. pp. 514–522.
- Li, Z., Wang, C., Han, M., Xue, Y., Wei, W., Li, L.J., Fei-Fei, L., 2018. Thoracic disease identification and localization with limited supervision, in: Proceedings of the IEEE conference on computer vision and pattern recognition, pp. 8290–8299.
- Matsuura, T., 2023. 2019 gastrointestinal cancer screening national aggregate report (in japanese). *Journal of Japanese Society of Gastroenterology (Nippon Shokakibyo Gakkai Zasshi)* 61, 86–101. doi:10.11404/jsgcs.61.86.
- Meng, L., Dong, D., Chen, X., Fang, M., Wang, R., Li, J., Liu, Z., Tian, J., 2020. 2d and 3D ct radiomic features performance comparison in characterization of gastric cancer: a multi-center study. *IEEE journal of biomedical and health informatics* 25, 755–763.
- Minemoto, T., Odama, S., Saitoh, A., Isokawa, T., Kamiura, N., Nishimura, H., Ono, S., Matsui, N., 2010. Detection of tumors on stomach wall in X-ray images, in: International Conference on Fuzzy Systems, pp. 1–5. doi:10.1109/FUZZY.2010.5584879.
- Nagano, N., Matsuo, T., 2010. Computer-aided diagnosis of gastrointestinal radiographs using adaptive differential filter and level set method, in: Proceedings of the 2010 International Conference on Modelling, Identification and Control, IEEE. pp. 442–447.
- Okamoto, H., Cap, Q.H., Nomura, T., Iyatomi, H., Hashimoto, J., 2019. Stochastic gastric image augmentation for cancer detection from X-ray images, in: 2019 IEEE International Conference on Big Data (Big Data), IEEE. pp. 4858–4863.
- Qian, N., 1999. On the momentum term in gradient descent learning algorithms. *Neural Networks* 12, 145–151.
- Rawla, P., Barsouk, A., 2019. Epidemiology of gastric cancer: global trends, risk factors and prevention. *Przegląd Gastroenterol* 14, 26–38.
- Redmon, J., Farhadi, A., 2018. YOLOv3: An incremental improvement. arXiv preprint arXiv:1804.02767.
- Ren, S., He, K., Girshick, R., Sun, J., 2015. Faster R-CNN: Towards real-time object detection with region proposal networks. *Advances in neural information processing systems* 28.

- Roder, D.M., 2002. The epidemiology of gastric cancer. *Gastric cancer* 5, 5–11.
- Shibata, T., Teramoto, A., Yamada, H., Ohmiya, N., Saito, K., Fujita, H., 2020. Automated detection and segmentation of early gastric cancer from endoscopic images using mask r-cnn. *Applied Sciences* 10, 3842.
- Shrivastava, A., Gupta, A., Girshick, R., 2016. Training region-based object detectors with online hard example mining, in: *Proceedings of the IEEE Conference on Computer Vision and Pattern Recognition*, pp. 761–769.
- Smirnov, E., Melnikov, A., Oleinik, A., Ivanova, E., Kalinovskiy, I., Luckyanets, E., 2018. Hard example mining with auxiliary embeddings, in: *Proceedings of the IEEE Conference on Computer Vision and Pattern Recognition Workshops*, pp. 37–46.
- Tan, M., Le, Q., 2019. EfficientNet: Rethinking model scaling for convolutional neural networks, in: *International Conference on Machine Learning*, pp. 6105–6114.
- Tan, M., Pang, R., Le, Q.V., 2020. EfficientDet: Scalable and efficient object detection, in: *Proceedings of the IEEE/CVF conference on computer vision and pattern recognition*, pp. 10781–10790.
- Tang, Y.B., Yan, K., Tang, Y.X., Liu, J., Xiao, J., Summers, R.M., 2019. Uldor: a universal lesion detector for ct scans with pseudo masks and hard negative example mining, in: *2019 IEEE 16th International Symposium on Biomedical Imaging (ISBI 2019)*, IEEE. pp. 833–836.
- Togo, R., Yamamichi, N., Mabe, K., Takahashi, Y., Takeuchi, C., Kato, M., Sakamoto, N., Ishihara, K., Ogawa, T., Haseyama, M., 2019. Detection of gastritis by a deep convolutional neural network from double-contrast upper gastrointestinal barium X-ray radiography. *Journal of gastroenterology* 54, 321–329.
- Uemura, N., Okamoto, S., Yamamoto, S., Matsumura, N., Yamaguchi, S., Yamakido, M., Taniyama, K., Sasaki, N., Schlemper, R.J., 2001. Helicobacter pylori infection and the development of gastric cancer. *New England journal of medicine* 345, 784–789.
- Wang, C.Y., Bochkovskiy, A., Liao, H.Y.M., 2023. YOLOv7: Trainable bag-of-freebies sets new state-of-the-art for real-time object detectors, in: *Proceedings of the IEEE/CVF Conference on Computer Vision and Pattern Recognition*, pp. 7464–7475.
- Wu, L., Zhou, W., Wan, X., Zhang, J., Shen, L., Hu, S., Ding, Q., Mu, G., Yin, A., Huang, X., et al., 2019. A deep neural network improves endoscopic detection of early gastric cancer without blind spots. *Endoscopy* 51, 522–531.
- Zhang, K., Zhang, Z., Li, Z., Qiao, Y., 2016. Joint face detection and alignment using multitask cascaded convolutional networks. *IEEE Signal Processing Letters* 23, 1499–1503.
- Zhang, Z., Guo, Y., Lu, Y., Li, S., 2019. Detection of metastatic lymph nodules in gastric cancer using deep convolutional neural networks, in: *2019 IEEE/ASME International Conference on Advanced Intelligent Mechatronics (AIM)*, IEEE. pp. 942–947.